Symposium Program

HYPERVELOCITY IMPACT SOCIETY

15th Hypervelocity Impact Symposium

April 14–19, 2019 | Destin, Florida

Table of Contents

Welcome to the 15th HVIS 2019 Symposium

William P. Schonberg
PhD, DS
President
Hypervelocity
Impact Society

On behalf of the Hypervelocity Impact Society, it is my pleasure to welcome you to our main event – the 2019 Hypervelocity Impact Symposium (HVIS 2019).

This is the 15th time we have held this forum on recent advances in the science and technology of hypervelocity impact phenomena and related technical areas. HVIS 2019 continues our longstanding international venue for the discussion, interchange, presentation and recognition of technical contributions to the field. The technical quality of the papers continues to be very high, with a diversity of topics ranging from Armor and Ballistic Technology to Equation of State to Spacecraft Orbital Debris Shielding. Your HVIS Board of Directors and the Conference Planning Committees have worked hard to bring a high-quality, rewarding science and engineering forum to the beautiful City of Destin, Florida. I especially wish to thank the Symposium Committee and Technical Chairs for their diligence and time spent in preparing HVIS 2019, its social activities, Companion Program, and the Symposium Proceedings.

Finally, congratulations! You now have membership in the Hypervelocity Impact Society from now until HVIS 2021. You are invited to visit your Society website at www.hvis.org, and please do not hesitate to let us know if you wish to volunteer on one of the Society's many committees.

William P. Schonberg, PhD, DS
President of Hypervelocity Impact Society

Welcome to HVIS 2019

David Littlefield
HVIS 2019
Symposium Chair

Welcome to the 2019 Hypervelocity Impact Symposium! This is the 15th symposium in the most recent series of symposia devoted to the study of hypervelocity impact phenomena and related technologies. The technical papers presented this week reaffirm the society's commitment to providing a forum for the continued interaction of international scientists, engineers, and industrialists. Our objective this week is to facilitate the discussion and exchange of technical information related to hypervelocity impact phenomenology.

The presentations of the Distinguished Scientist Award recipient and the Society's Best Paper Award reinforce the society's commitment to recognize and encourage excellence and quality in our fields of endeavor. The plenary session presentations and the symposium banquet's keynote address are also indicative of the broad range of interests held by society members. The excellent technical program and commercial exhibits of this symposium present an outstanding opportunity for everyone to be enriched by one another's expertise.

The presentations of the Distinguished Scientist Award recipient and the Society's Best Paper Award reinforce the society's commitment to recognize and encourage excellence and quality in our fields of endeavor.

Learn about and discuss the latest technical work in a wide variety of subject areas, network with your colleagues, make new friends, renew acquaintances, shop and compare the latest in impact-related equipment, software capabilities, and services offered by the companies in the Exhibit Hall – you are encouraged to take advantage of all this symposium has to offer. Also, please take a moment to visit with this year's cohort of Alex Charters Student Scholars. These fine young men and women are our future – please congratulate them on their selection this year and offer them your support and encouragement as future hypervelocity impact scientists and engineers.

We would like to take a moment to thank the following individuals and groups who volunteered their time and expertise to make this symposium a reality: the hypervelocity impact society board of directors, society committee chairs and committee members, the technical program chair, and the members of the HVIS 2019 technical program committee. Without your hard work, this symposium would not have been possible. The society thanks each of you for enriching our symposium with your presence and participation.

Enjoy your stay in Destin, and please do take the time to visit some of the local attractions. We are looking forward to personally meeting and greeting many of you throughout the next few days.

David Littlefield
HVIS 2019 Symposium Chair

UAB SCHOOL OF ENGINEERING
Knowledge that will change your world

HVIS 2019 is coordinated by the Department of Mechanical Engineering at the University of Alabama at Birmingham.

LEARN MORE
Email: sswatson@uab.edu
Phone: (205) 934-8460
Web: uab.edu/engineering/me
Mail: BEC 257
1150 10th Ave South
Birmingham, AL 35228

Exhibitors

Stop by the Exhibit Hall during the Symposium to visit with vendors about the latest in impact-related equipment, services and software capabilities.

CORDIN SCIENTIFIC IMAGING

Photron

coherent solutions
complexity made simple.

CertaSim

IX Cameras

AMO tronics

nac IMAGE TECHNOLOGY

PHANTOM AMETEK MATERIALS ANALYSIS DIVISION

SPECIALISED IMAGING

pco.

Schedule at a Glance

All technical sessions held in Emerald Ballroom

Sunday, April 14

5:00 pm Registration - *Lobby*
7:00 pm Welcome Reception - *Beachside Deck*

Monday, April 15

7:00 am Registration & Breakfast - *Emerald Foyer*
8:00 am Opening Ceremonies - *Emerald Ballroom*
8:40 am Distinguished Scientist Keynote - *Emerald Ballroom*
9:30 am Break - *Emerald Foyer*
9:50 am **Technical Session 1:**
High Velocity Penetration and Target Response I
Session Chairs: Angela Diggs and Sidney Chocron
11:30 am Lunch - *Emerald D,E*
12:30 pm **Technical Session 2:**
Material Response I
Session Chairs: James Cazamias and Dave Crawford
2:30 pm Break - *Emerald Foyer*
2:50 pm **Technical Session 3:**
Hypervelocity Phenomenology
Session Chairs: Mike Burkett and Erkai Watson
4:30 pm Technical Sessions End
5:30 pm Dinner Cruise - *Baytowne Wharf*

Tuesday, April 16

7:00 am Registration & Breakfast - *Emerald Foyer*
8:00 am **Keynote Session I** - *Emerald Ballroom*
Speaker: Werner Arnold
8:40 am **Exhibitor Briefings** - *Emerald Ballroom*
10:20 am Break - *Emerald Foyer*
10:40 am **Poster Session** - *Pelican Room*
12:00 pm Lunch - *Seagars Main Room*
1:00 pm Technical Sessions End
Board of Directors Committee Meeting - *Heron Room*
7:00 pm Beach S'mores Bonfire - *Sandestin Hilton Beach*

Wednesday, April 17

7:00 am Registration & Breakfast - *Emerald Foyer*
8:00 am **Technical Session 4:**
Spacecraft Meteoroid and Debris Shielding I
Session Chairs: Joel Williamsen and Phillip Mulligan
9:40 am Break - *Emerald Foyer*

10:00 am **Technical Session 5:**
High Velocity Penetration and Target Response II
Session Chairs: Shannon Ryan and Werner Arnold
12:00 pm Lunch - *Emerald D,E*
1:00 pm **Technical Session 6:**
Armor/Anti-Armor and Ballistic Technology
Session Chairs: Todd Bjerke and Brett Sorenson
2:40 pm Break - *Emerald Foyer*
3:00 pm **Technical Session 7:**
Fracture and Fragmentation
Session Chairs: David Price and Mike Hopson
5:00 pm Technical Sessions End
6:00 pm **Symposium Banquet** - *Emerald Ballroom*
Speaker: John Olivas, PhD

Thursday, April 18

7:00 am Registration & Breakfast - *Emerald Foyer*
8:00 am **Keynote Session II** - *Emerald Ballroom*
Speaker: Peter Sable
8:40 am **Technical Session 8:**
Analytical and Numerical Methodologies I
Session Chairs: Josh Miller and Justin Sweitzer
10:20 am Break - *Emerald Foyer*
10:40 am **Technical Session 9:**
Asteroid Impact and Planetary Defense
Session Chairs: Gene Hertel and George Flynn
12:20 pm Lunch - *Emerald D,E*
1:20 pm **Technical Session 10:**
Material Response II
Session Chairs: Scott Alexander and Nobuaki Kawai
3:00 pm Break - *Emerald Foyer*
3:20 pm **Technical Session 11:**
High Velocity Launchers
Session Chairs: Casey Uhlig and Sikhanda Satapathy
4:40 pm Technical Sessions End

Friday, April 19

7:00 am Registration & Breakfast - *Emerald Foyer*
8:00 am **Technical Session 12:**
Spacecraft Meteoroid and Debris Shielding II
Session Chairs: James Walker and Rohan Banton
9:40 am Break - *Emerald Foyer*
10:00 am **Technical Session 13:**
Analytical and Numerical Methodologies II/
Material Response III
Session Chairs: Kent Danielson and Brooke Corbett
12:00 pm HVIS Business meeting (box lunches served)
1:00 pm Symposium Adjourns

Organizing Committee

Symposium Chair:
David Littlefield, *The University of Alabama at Birmingham*

Technical Program Chair:
Geremy Kleiser, *Air Force Research Laboratory*

Exhibits Chair:
William Reinhart, *Sandia National Laboratory*

Conference Coordination:
Coordinator: Michelle Wiginton, *Missouri S&T*
Secretary: Tammy Mace, *Missouri S&T*

Board of Directors:
President: William Schonberg, *Missouri S&T*
Secretary-Treasurer: James Wilbeck, *Dynetics*
Past President: Todd Bjerke, *ASA/LT*
David Littlefield, *The University of Alabama at Birmingham*
Mark Burchell, *University of Kent*
Kathryn Harriss, *University of Kent*
William Reinhart, *Sandia National Laboratories*
Shannon Ryan, *Defense Science and Technology Organization*

Committee Chairs:
Membership Committee:
Brooke Myers Corbett, *Institute for Defense Analyses*
Nominations Committee:
Andrew Tonge, *Army Research Laboratory*
Awards Committee:
Josh Miller, *The University of Texas at El Paso*
Education Outreach Committee: John Borg, *Marquette University*
Communications Committee: James Walker, *Southwest Research Institute*
Site Selection Committee: Gene Hertel, *Sandia National Laboratory*

Technical Program Committee:
Andrew Tonge, *Army Research Laboratory*
Angela Diggs, *Air Force Research Laboratory*
Brett Sorenson, *Army Research Laboratory*
Casey Uhlig, *Army Research Laboratory*
David Crawford, *Crawford Technical Services*
David Lambert, *Air Force Research Laboratory*
David Price, *Atomic Weapons Establishment*
Eric Christiansen, *National Aeronautics and Space Administration*
Gene Hertel, *Sandia National Laboratories*
James Cazamias, *Army Research Laboratory*
James Walker, *Southwest Research Institute*
John Niederhaus, *Sandia National Laboratories*
Josh Miller, *The University of Texas at El Paso*
Joel Williamsen, *Institute for Defense Analyses*
Kent Danielson, *Engineer Research and Development Center*
Michael Hopson, *Naval Surface Warfare Center*
Michael Burkett, *Los Alamos National Laboratory*
Philip Mulligan, *Missouri S&T*
Rohan Banton, *Army Research Laboratory*
Scott Alexander, *Sandia National Laboratories*
Sidney Chocron, *Southwest Research Institute*
Shannon Ryan, *Defense Science and Technology Organization*
Sikhanda Satapathy, *Army Research Laboratory*
Tracy Vogler, *Sandia National Laboratories*
Todd Bjerke, *ASA/LT*
Wayne Chen, *Purdue University*

Symposium Schedule

Sunday Evening, April 14, 2019

5:00 pm – 7:30 pm
Registration - *Lobby*

7:00 pm
Welcome Reception - *Beachside Deck*

Monday Morning, April 15, 2019 | Emerald Ballroom | *Session Abstracts pp 16-17*

7:00 am
Registration & Breakfast

8:00 am – 8:40 am
Opening Ceremonies

8:40 am – 9:30 am
Distinguished Scientist Keynote Address

9:30 am – 9:50 am
Break - *Emerald Foyer*

9:50 am – 11:30 am
Technical Session 1: High Velocity Penetration and Target Response I

11:30 am – 12:30 pm
Lunch - *Emerald D, E*

Technical Session 1 | 9:50 am – 11:30 am | Emerald Ballroom

High Velocity Penetration and Target Response I

Session Chairs: Angela Diggs and Sidney Chocron

046 – An Analytical Model for Local Penetration of Ultra-high Molecular Weight Polyethylene Composite
Long H. Nguyen, Shannon Ryan, Adrian C. Orifici, and Stephen Cimpoeru

105 – Optimized Impact Mitigation Barriers for Insensitive Munitions Compliance of a 120mm Warhead
Kevin T. Miers, Daniel L. Prillaman, and Nausheen M. Al-Shehab

011 – In-situ Observation of Damage Evolution in Polycarbonate Subjected to Hypervelocity Impact
Nobuaki Kawai, Mikio Nagano, Sunao Hasegawa, and Eiichi Sato

080 – Automatic Mesh-Generation (FEM/SPH) for HVI-Simulations of Arbitrary Rotational Symmetric Impactors
Marvin Becker, Marina Seidl, Miriam Mehl, and Mhamed Souli

108 – Experiment Guided Simulation of Multi-Fragment Impact into PBXs
Andrew M. Schmalzer, John D. Yeager, Patrick R. Bowden, Daniel R. Guildenbecher, and Joseph D. Olles

Symposium Schedule

Monday Afternoon, April 15, 2019 | Emerald Ballroom | *Session Abstracts pp 17-19*

12:30 pm – 2:30 pm
Technical Session 2:
Material Response I

2:30 pm – 2:50 pm
Break - *Emerald Foyer*

2:50 pm – 4:30 pm
Technical Session 3:
Hypervelocity Phenomenology

4:30 pm
Technical Sessions End

5:30 pm
Dinner Cruise - *Baytowne Wharf*

Technical Session 2 | 12:30 pm – 2:30 pm

Material Response I

Session Chairs: James Cazamias and Dave Crawford

012 – Bayesian Model Selection for Metal Yield Models in High-velocity Impact
Teresa Portone, John Niederhaus, Jason Sanchez, and Laura Swiler

031 – Equation of State of Lead Filled Glass
Bernardo Farfan, William Reinhart, and Scott Alexander

040 – Modelling the Deformation of a High-hardness Armor Steel in Taylor Rod-on-anvil Experiments
Shannon Ryan, Brodie McDonald, Nikki Scott, Rory Bigger, Long Nguyen, and Sidney Chocron

083 – Thin Film Graded Density Impactors for High Rate Off-Hugoniot Loading: Application to Ta Strength
J. L. Brown, D. P. Adams, C. S. Alexander, J. L. Wise, and W. D. Reinhart

008 – High Velocity Impact of an Fe/Cr/Mn/Ni High Entropy Alloy
M. Cameron Hawkins, Sarah Thomas, Robert Hixson, Nan Li and Saryu Fensin

113 – Investigating Pressure Wave Impact on a Surrogate Head Model Using Numerical Simulation Techniques
Rohan Banton, Thuvan Piehler, Nicole Zander, Richard Benjamin, Josh Duckworth, and Oren Petel

Technical Session 3 | 2:50 pm – 4:30 pm

Hypervelocity Phenomenology

Session Chairs: Mike Burkett and Erkai Watson

030 – Experiments Using a Light Gas Gun to Investigate the Impact Melting of Gunshot Residue Analogues
V. Spathisa and M. C. Price

015 – Development of ARL's Multi-Energy Flash Computed Tomography Diagnostic: Capability to Track Mass-Flux through a Reconstruction Volume
Michael B. Zellner, Melissa S. Love, and Kyle Champley

035 – Four-View Split-Image Fragment Tracking in Hypervelocity Impact Experiments
Erkai Watson, Nico Kunert, Robin Putzar, Hans-Gerd Maas, and Stefan Hiermaier

112 – X-ray Diffraction Diagnostic Paired with Gas Gun Driven Compression of Polyethylene
Rachel C. Huber, Erik B. Watkins, Dana M. Dattelbaum, and Richard L. Gustavsen

077 – Hypervelocity Sequenced Laser Shadowgraph Instrument and Measurement of Debris Cloud with Hypervelocity
Ke Fawei, Huang Jie, Song Qiang, Wen Xuezhong, Li Xin, Xie Aimin, Li Jing, Jiang Lin, and Liu Sen

Symposium Schedule

Tuesday, April 16, 2019 | Emerald Ballroom

7:00 am
Registration & Breakfast

8:00 am – 8:40 am
Keynote Session I
Speaker: Werner Arnold

8:40 am – 10:20 am
Exhibitor Briefings
- *Emerald Ballroom*

10:20 am – 10:40 am
Break - *Emerald Foyer*

10:40 am – 1:00 pm
Poster Session*
- *Pelican Room*
*Denotes Poster. (All poster abstracts located in Technical Session Section for each category.)

12:00 pm – 1:00 pm
Lunch
- *Seagars Main Room*

1:00 pm
Technical Sessions End

7:00 pm
Beach S'mores Bonfire

Exhibitor Briefings | 8:40 am – 10:20 am

Hypervelocity Impact on a Laptop Computer: 130 Million Particle Model with the IMPETUS γSPH Solver
CertaSIM, LLC

Recent Advances in Ultra-High-Speed Imaging and Sensor Development
Specialised Imaging

Cordin Solutions for High-Speed Imaging
Cordin Scientific Imaging

Data Fusion and Signals Control in Ultrahigh Speed Ballistics Imaging
AMETEK / VISION

The Range of Applications of High-Speed and Ultra High-Speed Digital Video
HADLAND/ SHIMADZU/ IX

Prezise Real-time in-the-loop Control for Hypervelocity Applications
Amotronics

The New NAC Memrecam ACS-The World's First 40 Gigapixel Per Second High Speed Video Camera
NAC

An Introduction to Photron High-Speed Cameras
Photron

New High Speed Intensified Camera Based on sCMOS Sensor Technology
PCO Americas

Photonic Doppler Velocimetry- A Favored Approach in Optical Velocimetry Over VISAR and Fabry-Perot
Coherent Solutions Limited

Keynote Session I

Tuesday, April 16, 2019
8:00 am – 8:40 am

Speaker: Werner Arnold

Presentation Title:

Filling the Gap between Hypervelocity and Low Velocity Impacts

Authors: Werner Arnold, Thomas Hartmann, and Ernst Rottenkolber

Abstract: During more than one decade of studying initiation phenomenology numerous papers were published by the authors. A multitude of experimental data on hypervelocity impact initiation of plastic bonded high explosive charges by shaped charge jets (SCJ) and some data in the ordnance velocity impact regime obtained with STANAG projectiles and explosively formed projectiles (EFP) were generated. Amongst other findings the results showed that the established assumption that the critical stimulus is constant was wrong and that a new initiation model is needed taking the new results into account. Towards such a new model further investigation was necessary trying to make a link between the initiation phenomenology of shaped charge jet impacts in the hypervelocity regime and of projectile impacts in the lower velocity regime. To bridge the existing data gap a new approach was taken applying newly designed "simplified shaped charges" (SSC). This paper describes the way to this new approach and summarizes the related test results as well as their implications.

Symposium Schedule

Wednesday Morning, April 17, 2019 | Emerald Ballroom | *Session Abstracts pp 19-21*

7:00 am
Registration & Breakfast

8:00 am – 9:40 am
Technical Session 4:
Spacecraft Meteoroid and Debris Shielding I

9:40 am – 10:00 am
Break - *Emerald Foyer*

10:00 am – 12:00 pm
Technical Session 5:
High Velocity Penetration and Target Response II

12:00 pm – 1:00 pm
Lunch - *Emerald D, E*

Technical Session 4 | 8:00 am – 9:40 am

Spacecraft Meteoroid and Debris Shielding I

Session Chairs: Joel Williamsen and Phillip Mulligan

048 – Investigation on Response of an Aluminum Honeycomb Subjected to Hypervelocity Impacts using Lagrange and SPH for Numerical Modeling
Kumi Nitta, Masumi Higashide, Mirai Sueki, and Atushi Takeba

099 – Explosion of Hydrazine Tanks Due to Space Debris Impacts
Jérôme Limido, Christian Puillet, and Jean-Paul Vila

118 – Hypervelocity Impact of PrintCast A356/316L Composites
Lauren L. Poole, Manny Gonzales, Matthew R. French, William A. Yarberry III, and Zachary C. Cordero

066 – Using the DebriSat Fragments to Update the NASA Standard Satellite Breakup Model and Shape Effects on Ballistic Limit Equations
Heather Cowardin, Phillip Anz-Meador, James Murray, J.-C. Liou, Eric Christiansen, Marlon Sorge, Norman Fitz-Coy, and Tom Huynh

044 – Simulation Study of Non-spherical, Graphite-epoxy Projectiles
Joshua E. Miller

Technical Session 5 | 10:00 am – 12:00 pm

High Velocity Penetration and Target Response II

Session Chairs: Shannon Ryan and Werner Arnold

104 – High Velocity Impact Testing for Evaluation of Intermetallic Projectiles
Kevin J. Hill, Colt Cagle, Connor Woodruff, Michelle L. Pantoya, Joseph Abraham, and Casey Meakin

014 – Towards a Better Understanding of Shaped Charge Jet Formation and Penetration
David W. Price, Ernest J. Harris, and Frances G. Daykin

036 – Prediction of Micrometeoroid Damage to Lunar Construction Materials using Numerical Modeling of Hypervelocity Impact Events
Maria I. Allende, Joshua E. Miller, B. Alan Davis, Eric L. Christiansen, Michael D. Lepech, and David J. Loftus

119 – A Predictive Non-Dimensional Scaling Law for the Plate Perforation of Several Aluminum Alloys by Fragment-Simulating Projectiles
Weinong Chen and Zherui Guo

063 – Modeling Hypervelocity Impact of Reinforced Carbon-Carbon Composite Thermal Protection System
Alexander J. Carpenter, Sidney Chocron, and James D. Walker

023 – Dynamic Fragmentation of Boron Carbide with Laser-Driven Impact
Debjoy D. Mallick and KT Ramesh

Symposium Schedule

Wednesday Afternoon, April 17, 2019 | Emerald Ballroom | *Session Abstracts pp 21-24*

1:00 pm – 2:40 pm
Technical Session 6:
Armor/Anti-Armor and Ballistic Technology

2:40 pm – 3:00 pm
Break - *Emerald Foyer*

3:00 pm – 5:00 pm
Technical Session 7:
Fracture and Fragmentation

5:00 pm
Technical Sessions End

6:00 pm
Symposium Banquet Dinner
Banquet Speaker:
John Olivas, PhD
- *Emerald Ballroom*

Technical Session 6 | 1:00 pm – 2:40 pm **Technical Session 7 | 3:00 pm – 5:00 pm**

Armor/Anti-Armor and Ballistic Technology

Session Chairs: Todd Bjerke and Brett Sorenson

093 – Effect of Liquid Parameters on Protective Performance of Liquid Composite Target Subjected to Jet
Tan Yaping, Jia Xin, Huang Zhengxiang, Cai Youer, and Zu Xudong

050 – Defeating Modern Armor and Protection Systems
Markus Graswald, Raphael Gutser, Jakob Breiner, Florian Grabner, and Timo Lehmann

110 – 3D Printed Conical Shaped Charge Performance
Phillip Mulligan, Catherine Johnson, Jason Ho, Cody Lough, and Edward Kinzel

004 – Calculation of Jet Characteristics from Hydrocode Analysis
Justin C. Sweitzer, Scott D. Hill, and Nicholas R. Peterson

Fracture and Fragmentation

Session Chairs: David Price and Mike Hopson

061 – Assessment and Validation of Collision "Consequence" Method of Assessing Orbital Regime Risk Posed by Potential Satellite Conjunctions
Travis F. Lechtenberg and Matthew D. Hejduk

Fracture and Fragmentation (continued)

Session Chairs: David Price and Mike Hopson

097 – Characterization of the Ballistic Properties of Ejecta from Laser Shock-loaded Samples Using High Resolution ps Laser Imaging
Arnaud Sollier and Emilien Lescoute

120 – Conical Impact Fragmentation Test (CIFT)
Christopher Neel, Peter Sable, Philip Flater, and David Lacina

022 – Bulking as a Mechanism in the Failure of Advanced Ceramics
Brendan M. L. Koch, Calvin Lo, Tomoko Sano, and James David Hogan

056 – The Role of Inclusions in the Failure of Boron Carbide Subjected to Impact Loading
Andrew L. Tonge and Brian E. Schuster

089 – Pagosa Simulation of Hypervelocity Impact and Fragmentation from Hypersonic Explosions
Xia Ma, David Culp, and Brandon Smith

025 – Deformation and Acceleration of Zn and Cu Liners under Explosive Shock Loading
Puwadet Sutipanya, Fumikazu Saito, Mitsuyori Nakashita, Takashi Ogino, Yutaka Takizawa, Yohsuke Okada, and Masahiko Natsubori

Symposium Banquet Dinner

Wednesday Evening, April 17, 2019 | 6:00 pm – 8:00 pm | Emerald Ballroom

Banquet Presentation and Speaker:

Inventing Hypersonic Flight

Richard P. Hallion, PhD

Senior Adviser for Air and Space Issues, Directorate for Security, Counterintelligence and Special Programs Oversight, *The Pentagon, Washington, D.C.*

Richard P. Hallion is a Trustee of Florida Polytechnic University. He also serves as an advisor to the Royal Air Force Centre for Air Power Studies (RAF-CAPS) and as a consultant to various organizations, including the Mitchell Institute of the Air Force Association, and the Science and Technology Policy Institute (STPI) of the Institute for Defense Analyses (IDA). Previously, Dr. Hallion was a founding museum curator at the National Air and Space Museum of the Smithsonian Institution; served as a Historian with the National Aeronautics and Space Administration and the U.S. Air Force; held the General Harold Keith Johnson Chair of Military History at the U.S. Army War College; ran the USAF History and Museums Program; and was a senior advisor on aerospace technology and policy for the Secretary of the Air Force.

He has flying experience as a mission observer (not pilot) in a wide range of military and civil aircraft, and is a Fellow of the American Institute of Aeronautics and Astronautics, the Royal Aeronautical Society, and the Royal Historical Society.

Dr. Hallion received a Ph.D in history from the University of Maryland, and completed postgraduate executive study programs at the Federal Executive Institute and the John F. Kennedy School of Government at Harvard University. He has served on several study panels for the Air Force Studies Board and the National Academies of Science, Engineering, and Medicine projects, including defense against future high-speed threats and meeting future Air Force Science, Technology, Engineering, and Mathematics (STEM) workforce needs.

Symposium Schedule

Thursday Morning, April 18, 2019 | Emerald Ballroom | *Session Abstracts pp 24-26*

7:00 am
Registration & Breakfast

8:00 am – 8:40 am
Keynote Session II
Speaker: Peter Sable
- *Emerald Ballroom*

8:40 am – 10:20 am
Technical Session 8:
Analytical and Numerical Methodologies I

10:20 am – 10:40 am
Break - *Emerald Foyer*

10:40 am – 12:20 pm
Technical Session 9:
Asteroid Impact and Planetary Defense

12:20 pm – 1:20 pm
Lunch - *Emerald D, E*

Keynote Session II

Thursday, April 18, 2019
8:00 am – 8:40 am

Speaker: Peter Sable

Presentation Title:

High Strain-rate Shear and Friction Characterization of Fully-Dense Polyurethane

Authors: Peter Sable, Christopher H. Neel, and John P. Borg

Abstract: A series of friction and constant-pressure oblique plate impact experiments were conducted in an effort to observe dynamic friction characteristics and shear strength behaviors of fully dense, high durometer polyurethane (PU). For both configurations, an angle-faced projectile was accelerated towards a target set at the same angle via slotted-barrel light-gas gun. Oblique impact resulted in high strain-rate (~105 s-1) combined normal and shear stress loading with magnitudes of approximately 0.9 and 0.2 GPa, respectively, depending on impact velocity and angle. Material response was inferred from rear free-surface particle velocities measured using transverse photon Doppler velocimetry techniques. Coefficients of friction were calculated from the ratios of shear to normal stress at the impact interface between a PU projectile and 7075-T6 aluminum target. Taking into account the slip speed as the difference between expected and observed transverse velocity, the coefficient of friction was ranged from 0.1 to 0.3 with an apparent inverse pressure dependence. Shear strengths were found to gradually increase with confining normal stress, greatly exceeding magnitudes seen by traditional low-rate tensile and shear testing. Additionally, a discussion on the role of adhesion is presented contrasting polymer-metal bond failure to intrinsic material failure.

Symposium Schedule

Thursday Morning, April 18, 2019 | Emerald Ballroom | *Session Abstracts pp 24-26*

Technical Session 8 | 8:40 am – 10:20 am

Analytical and Numerical Methodologies I

Session Chairs: Josh Miller and Justin Sweitzer

078 – An Accurate SPH Scheme for Hypervelocity Impact Modeling
Anthony Collé, Jérôme Limido , Thomas Unfer, and Jean-Paul Vila

090 – Analytically Derived Space Time-based Boundary Condition (STBC) to Account for Stress Wave Propagation in Heterogeneous Micromechanical Model at Hypervelocity Impact
Zhiye Lia and Somnath Ghosh

060 – Validation of an Improved Contact Method for Multi-Material Eulerian Hydrocodes in Three-Dimensions
Kenneth C. Walls and David L. Littlefield

111 – Higher-order Finite Elements for Lumped-Mass Explicit Modeling of High-speed Impacts
Kent Danielson, Bob Browning, and Mark Adley

091 – Multiscale Modeling of Reactive Structural Materials
Grant Smith, Scott Bardenhagen, and John Nairn

Technical Session 9 | 10:40 am – 12:20 pm

Asteroid Impact and Planetary Defense

Session Chairs: Gene Hertel and George Flynn

038 – Impact Modeling for the Double Asteroid Redirection Test (DART) Mission
Emma S. G. Rainey, Angela M. Stickle, Andrew F. Cheng, Andrew S. Rivkin, Nancy L. Chabot, Olivier S. Barnouin, Carolyn M. Ernst, and the AIDA/DART Impact Simulation Working Group

028 – Momentum Transfer in Hypervelocity Cratering of Meteorites and Meteorite Analogs: Implications for Asteroid Deflection
George J. Flynn, Daniel D. Durda, Mason J. Molesky, Brian A. May, Spenser N. Congram, Colleen L. Loftus, Jacob R. Reagan, Melissa M. Strait, and Robert J. Macke

032 – Simulations of Magnetic Fields Produced by Asteroid Impact: Possible Implications for Planetary Paleomagnetism
David A. Crawford

049 – Size Scaling of Crater Size, Ejecta Mass, and Momentum Enhancement due to Hypervelocity Impacts into 2024-T4 and 2024-T351 Aluminum
James D. Walker, Sidney Chocron, and Donald J. Grosch

059 – Hypervelocity Impact on Concrete and Sandstone: Momentum Enhancement from Tests and Hydrocode Simulations
Sidney Chocron, James D. Walker, Donald J. Grosch, Stephen R. Beissel, Daniel D. Durda, and Kevin R. Housen

Symposium Schedule

Thursday Afternoon, April 18, 2019 | Emerald Ballroom | *Session Abstracts pp 26-27*

1:20 pm – 3:00 pm
Technical Session 10:
Material Response II

3:00 pm – 3:20 pm
Break - *Emerald Foyer*

3:20 pm – 4:40 pm
Technical Session 11:
High Velocity Launchers

4:40 pm
Technical Sessions End

Technical Session 10 | 1:20 pm – 3:00 pm

Material Response II

Session Chairs: Scott Alexander and Nobuaki Kawai

020 – Statistics of Energy Dissipation in the Hypervelocity Impact Shock Failure Transition
Dennis Grady

042 – Dynamic Response of Graphene and yttria-stabilized Zirconia (YSZ) Composites
Christopher R. Johnson and John P. Borg

102 – Validating Ice Impacts Using Adaptive Smoothed Particle Hydrodynamics for Planetary Defense
Dawn Graninger, Megan Bruck Syal, J. Michael Owen, and Paul Miller

007 – Wave Speeds in Single and Polycrystalline Copper
Sarah A. Thomas, Robert S. Hixson, M. Cameron Hawkins, and Oliver T. Strand

027 – Study on Phase Transformation in Tin Under Dynamic Compression
Camille Chauvin, Frédéric Zucchini, Thierry D'Almeida, and David Palma de Barros

Technical Session 11 | 3:20 pm – 4:40 pm

High Velocity Launchers

Session Chairs: Casey Uhlig and Sikhanda Satapathy

016 – Electrically-Launched mm-sized Hypervelocity Projectiles
W. Casey Uhlig, Paul R. Berning, Peter T. Bartkowski, and Matthew J. Coppinger

039 – HyFIRE: Hypervelocity Facility for Impact Research at Johns Hopkins University
Gary Simpson, Matthew Shaeffer, and K.T. Ramesh

084 – The JHUAPL Planetary Impact Lab (PIL): Capabilities and Initial Results
R. Terik Daly, Olivier S. Barnouin, Andrew M. Lennon, Angela M. Stickle, Emma S. Rainey, Carolyn M. Ernst, and Andrew A. Knuth

117 – Timing Analysis of the Auxiliary Pump Technique to Improve the Performance of an Implosion-Driven Hypervelocity Launcher
Mafa Wang, Justin Huneault, Andrew J. Higgins, and Sen Liu

Symposium Schedule

Friday Morning, April 19, 2019 | Emerald Ballroom | *Session Abstracts pp 28-29*

7:00 am
Registration & Breakfast

8:00 am – 9:40 am
Technical Session 12:
Spacecraft Meteoroid and Debris Shielding II

9:40 am – 10:00 am
Break - *Emerald Foyer*

10:00 am – 12:00 pm
Technical Session 13:
Analytical and Numerical Methodologies II/Material Response III

12:00 pm – 1:00 pm
HVIS Business meeting
(box lunches served)
- *Emerald Ballroom/Foyer*

1:00 pm
Symposium Adjourns

Technical Session 12 | 8:00 am – 9:40 am

Spacecraft Meteoroid and Debris Shielding II

Session Chairs: James Walker and Rohan Banton

037 – Depth of Penetration Criteria on Metallic Surfaces for use in MMOD Risk Assessment
Henry Nahra, Louis Ghosn, Eric Christiansen, Joshua Miller, and Bruce A. Davis

071 – Numerical Study of Dynamic Behavior of Foams Subjected to High- to Hyper-velocity Impact
Xiaotian Zhang, Ruiqing Wang, and Q.M. Li

029 – Predicting Orbital Debris-induced Failure Risk of Wire Harnesses Using SPH Hydrocode Modeling
Joel Williamsen, Michael Squire, and Steven Evans

054 – Debris Risk Evolution and Dispersal (DREAD) for Post-fragmentation Modeling
Daniel L. Oltrogge and David A. Vallado

026 – A Rupture Limit Equation for COPVs Following a Perforating MMOD Impact
William P. Schonberg

Technical Session 13 | 10:00 am – 12:00 pm

Analytical and Numerical Methodologies II/ Material Response III

Session Chairs: Kent Danielson and Brooke Corbett

109 – Adiabatic Heating and Damage Formation of Composite Associated with High-velocity Impact
Zhiye Li, Xiaofan Zhang, Daniel J.O'Brien, and Somnath Ghosh

052 – A Mesoscale-based Statistical Mechanics Framework for Modeling, Homogenization and Uncertainty Quantification of Sand in Hydrocodes
Gerald Pekmezi and David L. Littlefield

017 – Mesoscale Modeling and Debris Generation in Hypervelocity Impacts
Stephanie N. Q. Bouchey and Jeromy T. Hollenshead

033 – Hypervelocity Penetration of Granular Silicon Carbide from Mesoscale Simulations
Brian J. Demaske and Tracy J. Vogler

072 – Numerical and Experimental Evaluations of a Glass-Epoxy Composite Material Under High Velocity Oblique Impacts
Christopher T. Key and C. Scott Alexander

010 – Effects of EOS and Constitutive Models on Simulating Copper Shaped Charge Jets in ALEGRA
Robert L. Doney, John H. J. Niederhaus, Timothy J. Fuller, and Matthew J. Coppinger

Technical Session 1:

High Velocity Penetration and Target Response I

(*denotes Poster Session)

046 – An Analytical Model for Local Penetration of Ultra-High Molecular Weight Polyethylene Composite

Long H. Nguyen, Shannon Ryan, Adrian C. Orifici, and Stephen Cimpoeru

A validated numerical model is used to investigate the penetration of ultra-high molecular weight polyethylene (UHMW-PE) composite under ballistic impact. It is shown that the boundary condition imposed on the back face of the composite target strongly influences the penetration mode at late time, and that this transition occurs upon the arrival of the compressive or release wave (generated at the target back face) to the projectile-target interface. For a target with a thickness that is semi-infinite, the model shows that penetration is resisted locally until the projectile comes to rest. An analytical model is proposed to describe this local penetration mode based on an axial momentum balance concept. The penetration model shows good agreement with numerical simulations for targets under local penetration.

105 – Optimized Impact Mitigation Barriers for Insensitive Munitions Compliance of a 120mm Warhead

Kevin T. Miers, Daniel L. Prillaman, and Nausheen M. Al-Shehab

The U.S. Army ARDEC at Picatinny Arsenal, NJ is working to develop technologies to mitigate the violent reaction of a 120mm warhead, loaded with an aluminized HMX-based enhanced blast explosive, when subjected to the NATO Insensitive Munitions (IM) Fragment Impact (FI) test. As per NATO STANAG 4496, FI testing is conducted at 2530±90 m/s with a 14.3mm diameter, L/D~1, 160˚ conical nosed mild steel fragment. Reaction violence resulting from FI can be mitigated by the use of liners or barriers applied to the munition itself or its packaging, commonly referred to as a Particle Impact Mitigation Sleeves (PIMS). Previous development efforts for this item focused on a lightweight plastic warhead support which was able to reduce the severity of the input shock sufficiently to prevent high order detonation. However, violent sub-detonative responses were still observed which occurred over several hundred microseconds, consumed part of the explosive charge, and ejected hazardous debris over large distances. These responses are driven by rapid combustion coupled with damage to the explosive as well as mechanical confinement. Quantitative modeling of these scenarios is a challenging active research area. Prior experimental results and modeling guidance have shown that mitigation of these reactions requires a more substantial reduction in the overall mechanical insult to the explosive. In particular, steel and aluminum PIMS have been able to efficiently provide the necessary fragment velocity reduction, breakup and dispersion in typical packaging applications. Packaged warheads were tested at the GD-OTS Rock Hill facility with several PIMS designs incorporated into the ammunition containers. Several designs were demonstrated to provide benign reactions with minimal added weight. Future iterations will attempt to further improve the design using advanced lightweight barrier materials.

011 – In-situ Observation of Damage Evolution in Polycarbonate Subjected to Hypervelocity Impact

Nobuaki Kawai, Mikio Nagano, Sunao Hasegawa, and Eiichi Sato

Hypervelocity-impact experiments have been performed on polycarbonate to investigate the impact-induced damage process progressing inside polymer material. The damage evolution and stress-wave propagation associated with hypervelocity impact have been observed by means of two imaging methods using ultra-high-speed cameras. First one is the two-directional (side-view and rear-view) scattered light imaging. The obtained time-resolved images provide the information about the three-dimensional time evolutions of not only damage development but also damage texture. Another one is the cross-polarized shadowgraph. In this measurement, the time evolution of stress field is clearly visualized. The results obtained in this study strongly indicate that the combination of various imaging methods that each one can provide different information is useful way to obtain the knowledge about the damage process and mechanism associated with hypervelocity impact.

080 – Automatic Mesh-Generation (FEM/SPH) for HVI-Simulations of Arbitrary Rotational Symmetric Impactors

Marvin Becker, Marina Seidl, Miriam Mehl, and Mhamed Souli

For the numerical description of high velocity impact, Smooth-Particle-Hydrodynamics (SPH) has gained more and more interest. The standard Lagrangian Finite-Element (FE) approach has difficulties in describing large deformations and fracture. However, a simulation based on SPH only is very expensive due to the small size of the particles. A well adopted solution to this is to couple both methods, using SPH only where it is necessary, and capturing the outer boundary conditions with a bias FE-mesh correctly - without considerable extra computational cost. We apply such a hybrid approach in LS-DYNA® for the characterization of threats in terminal ballistic. Different meshing approaches for the projectile and the target were implemented to guarantee an optimal initial condition. The particle size and the required size of the SPH-region were studied to exclude discretization effects. Exemplarily, a projectile surrogate with simplified geometry is investigated for a fixed impact velocity and two different angles of obliquity. A qualitative comparison between experiments, observed with X-ray cinematography, reveals a good potential of this approach towards predicting fracture and ricochet during high velocity impact events.

108 – Experiment Guided Simulation of Multi-Fragment Impact into PBXs

Andrew M. Schmalzer, John D. Yeager, Patrick R. Bowden, Daniel R. Guildenbecher, and Joseph D. Olles

Multi-fragment impact of energetic materials can provide the impetus initiation and growth to detonation when shockwaves from these discrete fragments collide. The Sandia hydrocode CTH is used with reactive burn modeling to identify relationships between spherical fragment separation distances, variable fragment arrival timing, and initiability in energetic materials. This work demonstrates that detonation is most likely to occur is when multiple fragments collide with a surface simultaneously, because of the cumulative pressure rise of two equal colliding waves compared to the colliding waves generated by fragment impacts offset in time.

068* – Comparison of the Hydrodynamic Ram Caused by Single and Two Projectiles Impacting Water-filled Containers

Yangziyi Ji, Xiangdong Li , Lanwei Zhou, and Xiaoying Lan

High-velocity impact on fluid-filled containers is a matter of interest in the studies of aircraft fuel tank vulnerability. The penetrator transfers its energy and momentum to the fluid and could damage the container, which is referred to as hydrodynamic ram (HRAM). Most of the conducted studies have addressed this problem by considering the single impact. However, the present study compared the hydrodynamic ram caused by single and two spherical projectiles impacting water-filled containers. To achieve the goal of accelerating two projectiles together, a special aluminum sabot was designed to hold two projectiles in a 25 mm ballistic gun. In the present paper, Arbitrary Lagrangian-Eulerian (ALE) methods in LS-DYNA was used to conduct the numerical simulation of this complex fluid-structure interaction problem. The comparison of the pressure histories, plate profiles between the experiment and simulation proved the validity of the numerical model. Then the experimentally verified finite element models were further used to investigate the differences between the single and double projectiles cases, such as the pressure profiles inside the water and the energy-time histories of various parts during different hydrodynamic ram phases.

070* – Study on Shaped Charged Jet Initiation of Solid Rocket Motors

Hao Cui, Rui Guo, Pu Song, Jinsheng Xu, Xiaohui Gu, and Rongzhong Liu

In order to study the mechanism of initiation of solid rocket motors under the impact of shaped charged jet, shaped charge jet initiation test of motors was experimentally studied to evaluate the safety of the motor under the accident attack in the battlefield environment. The experimental results indicated that motors had a detonation reaction under the shaped charge jet impact, of which the head velocity was more than 6000m/s. The response of a motor was recorded by high-speed photography. In addition, the mechanism of initiation of propellant charges was discussed by numerical simulations. Pressure-time and reaction-time of propellant were analyzed in this paper.

076* – Investigation on the Impact and Penetration Performance of the Particulated Jet into Concrete Targets

Qi-feng Zhu, Qiang-qiang Xiao, Zheng-xiang Huang, Xu-dong Zu, and Xin Jia

In this paper, the performance of the particulated jet impact and penetration into concrete targets were explored. Kinds of alloy materials, including titanium alloys (TC21, TC1), nickel-titanium (Ni-Ti) alloy and zirconium-niobium (Zr-Nb) alloy, were selected as the liner materials. X-ray experiments were carried out to evaluate the jetting behaviors. Depth of penetration (DOP) experiments were conducted. The cavity diameters, penetration depths and the parameters of the impact craters generated by the jets were analyzed. Data indicated that the particulated jet having a certain range of larger diameter caused more extensive damage to the surface of the concrete targets comparing with the coherent jet. The concrete matrix materials on the impact surfaces were pulverized. The penetration depth

resulting from the particulated jet decreased in some degree, but the cavity diameter increased significantly. Penetration efficiency varied because of the different degree of dispersion of the particulated jets, meaning which was sensitive to the stand-off distance.

082* – Effect of Size on Liquid-filled Compartment Structure Armor Resistant to Shaped Charge Jet

Xudong Zu, Zheng-Xiang Huang, Zhongwei Guan, and Yaping Tan

In this study, size effect on a liquid-filled compartment structure armor, which is resistant to shaped charge jet (SCJ), is investigated through theoretical and X-ray experiments. A model of the interaction between the liquid-filled structure armor and the SCJ is examined by analyzing the spread of shock waves when the jet penetrates the liquid, the effect of boundary constraint of the compartment and the liquid movement under the shock waves. Based on the theoretical model, the velocity range of the disturbed SCJ with compartment size is calculated and the best height of the compartment is reported. The experimental results validate the theoretical model, which can be used as a reference in the structural design of the liquid-filled compartment.

095* – Study on the Explosion-proof Performance of Polyurea-reinforced Masonry Walls with Different Spraying Methods

Wei Shang, Xu-dong Zu, Zheng-xiang Huang, and Wen-ni Shen

Based on the propagation theory of blast wave and the strain rate effect of polyurea, the explosion-proof performance of polyurea-reinforced masonry walls with different spraying methods was discussed in this paper. The impact fracture of masonry walls after contact explosion was analyzed, and the fracture results of blast wave on polyurea-reinforced masonry walls with different spraying methods were predicted. Furthermore, explosion-proof experiments of standard masonry wall (2m×1.2m×0.37m) under three conditions, including non-sprayed, back surface sprayed polyurea and double-sided sprayed polyurea, were carried out to verify the theoretical predictions. Finally, the impact fractures results of standard masonry walls after 1 kg TNT contact explosion under the three conditions were obtained. The test results were in good agreement with the theoretical predictions. It clearly demonstrated that polyurea coating can significantly improve the explosion-proof performance of the masonry walls, and double-sided sprayed showed better explosion-proof performance than back surface sprayed at the same coating thickness.

Keynote 1: 073 – Filling the Gap between Hypervelocity and Low Velocity Impacts

Werner Arnold, Thomas Hartmann, and Ernst Rottenkolber

During more than one decade of studying initiation phenomenology numerous papers were published by the authors. A multitude of experimental data on hypervelocity impact initiation of plastic bonded high explosive charges by shaped charge jets (SCJ) and some data in the ordnance velocity impact regime obtained with STANAG projectiles and explosively formed projectiles (EFP) were generated. Amongst other findings the results showed that the established assumption that the critical stimulus is constant was wrong and that a new initiation model is needed taking the new results into account. Towards such a new model further investigation was necessary trying to make a link between the initiation phenomenology of shaped charge jet impacts in the hypervelocity regime and of projectile impacts in the lower velocity regime. To bridge the existing data gap a new approach was taken applying newly designed "simplified shaped charges" (SSC). This paper describes the way to this new approach and summarizes the related test results as well as their implications.

Technical Session 2: Material Response I

(*denotes Poster Session)

012 – Bayesian Model Selection for Metal Yield Models in High-Velocity Impact

Teresa Portone, John Niederhaus, Jason Sanchez, and Laura Swiler

The shock hydrodynamics code ALEGRA and the optimization toolkit Dakota are used here to analyze the uncertainty in penetration data from a previous set of high-velocity impact experiments. The data are time-series observations of a long tungsten-alloy rod impacting a hardened steel plate at approximately 1250 m/s. Based on these data and their inferred uncertainty, calibrated and uncertainty-informed material parameters are developed for three competing steel yield models in ALEGRA. A Bayesian model selection procedure is devised to choose between the calibrated models in a systematic, automated fashion. The procedure is executed with ALEGRA and Dakota, finding that the Zerilli-Armstrong model provides optimal representation of the steel in the impact experiment.

031 – Equation of State of Lead Filled Glass

Bernardo Farfan, William Reinhart, and Scott Alexander

Equation of state properties were studied for the high-lead glass Corning 0120, which is a potash-soda-lead glass also referred to as G12. This glass, which contains approximately 30% PbO by weight and has a density, o, of 3.034 g/cm3 possesses properties suitable for many applications in industry such as optical components for space exploration instrumentation. Further understanding of its mechanical properties is desired for more complex applications in various fields, including applications where the glass may experience high-pressure shock loading. In this work plate impact experiments were conducted to determine the dynamic response of Corning 0120 at high stress levels. Tests were conducted over the pressure range from approximately 5 to 25 GPa utilizing the 90 mm bore single-stage powder driven gas gun at the Sandia National Laboratories STAR Facility. For this study, we used one-inch diameter Corning 0120 glass samples of two different thicknesses (3 mm and 7 mm) to use the evolution of the shock wave propagation through the material for analysis. The time-resolved material response was measured by means of a Velocity Interferometer System for Any Reflector system (VISAR). Results will be presented detailing the high-pressure shock loading response characteristics of the high-lead glass Coning 0120. Comparisons are made with similar results for lead free glass to assess the most prominent changes compared to lower density glasses and other lead filled glasses.

040 – Modelling the Deformation of a High-Hardness Armour Steel in Taylor Rod-on-anvil Experiments

Shannon Ryan, Brodie McDonald, Nikki Scott, Rory Bigger, Long Nguyen, and Sidney Chocron

A high hardness armour steel (HHA) has been extensively characterized under tension, compression, and shear loading at quasi-static and dynamic rates incorporating ambient and elevated temperatures. The resulting data has been used to derive constants for four plasticity constitutive models: Johnson-Cook (JC), Zerilli-Armstrong (ZA), modified Johnson-Cook (MJC), and a generalized J2-J3 yield surface (GYS). The resulting models have been used to predict the response of the HHA material during Taylor rod-on-anvil experiments. High speed photography and digital image correlation was used during the rod-on-anvil experiments to capture both transient deformation profiles and maximum principal strain along the surface of the rod (i.e. compression along the length of the rod). This data permits an in-depth evaluation of the numerical models, increasing the utility of the rod-on-anvil experiment as a constitutive model validation experiment. The JC, MJC, and GYS models were found to provide the best prediction of the shape of the rod (nose diameter and length), within 2% of the experimental measurement in all four rod-on-anvil experiments which did not result in fracture. The JC and GYS models, furthermore, were found to provide the best agreement with the measured transient surface strain profiles, predicting the experimental measurement to within 10% at all measurement locations and time steps for the experiment resulting in maximum deformation (impact velocity = 208 m/s). The results suggest that the added complexity of models such as the MJC and GYS, which incorporate strain hardening saturation, two-part strain rate dependency, and J3 plasticity effects, are unnecessary for HHA under the loading conditions experienced during rod-on-anvil experiments.

083 – Thin Film Graded Density Impactors for High Rate Off-Hugoniot Loading: Application to Ta Strength

J. L. Brown, D. P. Adams, C. S. Alexander, J. L. Wise, and W. D. Reinhart

Graded density impactors (GDIs) have long been of interest to provide off-Hugoniot loading capabilities for impact systems. We describe a new technique which utilizes sputter deposition to produce an approximately 40 m-thick film containing alternating layers of Al and Cu. The thicknesses of the respective layers are adjusted to give an effective density gradient through the film. The GDIs were launched into samples of interest with a 2-stage light gas gun, and the resulting shock-ramp-release velocity profiles were measured over timescales of ~10 ns with a new velocimetry probe. Results are shown for the direct impact of the film onto a LiF window, which allows for the dynamic characterization of the GDI, as well as from impact onto a thin (~40 m) sputtered Ta sample backed by a LiF window. These measurements were coupled into mesoscale numerical simulations to infer the strength of Ta at the high rate (107 s-1), and high pressure (1 MBar) conditions this unique capability provides. Initial results suggest this is a viable strength platform which fills a critical gap and aids in cross-platform comparisons with other high-pressure strength platforms.

008 – High Velocity Impact of a Fe/Cr/Mn/Ni High Entropy Alloy

M. Cameron Hawkins, Sarah Thomas, Robert Hixson, Nan Li, and Saryu Fensin

A series of shock loading experiments were conducted on High Entropy Alloy (HEA) samples consisting of Fe/Cr/Mn/Ni in weight percentages of 25.2/23.5/24.8/26.5. Characterizing this transition metal alloy is a first step in understanding the shock compression response of this relatively new class of alloy. A single stage light gas gun was used to conduct a series of flyer plate symmetric impact experiments to obtain fundamental dynamic properties. Photonic Doppler Velocimetry (PDV) diagnostics were employed to measure the free surface velocity on the back of each target during dynamic compression. These experiments yielded four data points that are in reasonable agreement with an estimated Hugoniot for the material.

113 – Investigating Pressure Wave Impact on a Surrogate Head Model Using Numerical Simulation Techniques

Rohan Banton, Thuvan Piehler, Nicole Zander, Richard Benjamin, Josh Duckworth, and Oren Petel

Primary blast wave impact on military personnel is of major concern particularly as it relates to mild traumatic brain injury. The current research is developing numerical models used to determine the appropriate volumetric and deviatoric response of a surrogate head subject to primary blast wave from an explosive. The simulated results revealed strong compressive loading in the anterior region of the surrogate brain resulting from frontal blast impact. The calculated results produced good agreement with experimental data in terms of the external pressure flow field that transverse the surrogate head and the intracranial pressure measurements in the brain-simulant. Simulated results also revealed elevated shear stress distribution at the skull/surrogate brain interface with more dominate forces appearing at the base (interface) of skull. The results from this study indicate the potential for shearing/tearing of brain tissue due to blast loading.

057* – Eulerian Hydrocode Modeling of a Dynamic Tensile Extrusion Experiment

M. W. Burkett

Eulerian hydrocode simulations using the Mechanical Threshold Stress (MTS) flow stress model were performed to provide insights into dynamic tensile extrusion experiments with copper (Cu) and tantalum (Ta). The extrusion of Cu and Ta projectiles was simulated with an explicit, two-dimensional Eulerian continuum mechanics hydrocode and compared with data to determine if this extrusion concept was a useful indirect hydrocode material strength model validation experiment. The data consisted of high-speed images of the extrusion process, PDV to measure the projectile velocity history, die transit time, dynamic temperature measurements of the extruded material, recovered extruded samples, and post-test metallography. The hydrocode was developed to predict large-strain and high-strain-rate loading problems. Some of the code features include a high-order advection algorithm, a material interface tracking scheme and a van Leer monotonic advection-limiting. The MTS model was utilized to evolve the flow stress as a function of strain, strain rate and temperature. Average strain rates on the order of 104 s-1 and plastic strains exceeding 300% were predicted in the extrusion of copper at impact velocities between 400 - 450 m/s, while plastic strains exceeding 800% were predicted for Ta. Quantitative comparisons between the predicted and measured deformation topologies and extrusion rate were made. Comparisons, using MTS, between the calculated and measured influence of the initial texture on the dynamic extrusion response of tantalum were performed. In the final version of the paper, comparisons between the predicted and measured projectile velocity profiles and die transits times (using PDV) and observed and measured temperatures will be compared. Also, comparisons for selected results obtained for Cu extrusion using MTS and Zerilli-Armstrong (Z-A) strength models will be provided. Finally, the feasibility of using the extruder experiment data to validate hydrocode strength models will be discussed.

Technical Session 3: Hypervelocity Phenomenology

(*denotes Poster Session)

030 – Experiments Using a Light Gas Gun to Investigate the Impact Melting of Gunshot Residue Analogues

V. Spathis and M. C. Price

In this set of experiments, the versatility of the University of Kent's light gas gun was utilized to obtain a selection of corroborative data regarding the formation and impact of metallic gunshot residues onto high purity silicon wafers. The results from the two experiments are presented. The first experiment investigated how the formation of metallic residues varied as gunshot residue analogues traversed through air under a range of pressures from 0.056 millibar (5.6 Pa) to 1 bar (100 kPa), using solely the energy released during primer ignition; the second involved firing a metallic powder mix of pre-determined composition (via a split-sabot) under vacuum at two velocities- 500 ms-1 and 2000 ms-1. This ensured that there was no ignition or heating of the powders, unlike the first experiment, and so the morphology of the particles collected would be solely due to impact. The residues on the substrates were then analyzed using a cold Field Emission Gun Scanning Electron Microscope (FEG) and Energy Dispersive X-ray (EDX) detector. By separating the ignition process of the primers from the residue impacts, it allows for a closer look into the formation of these particles and helps determine whether their varied morphologies are due to the heating caused during the activation and combustion of the primer or whether its due to impact melting. This information can aid in the understanding of metallic particle formation in different pressure environments and give insight into the physical state of firearm residues when they impact a surface. Hydrocode modelling was also incorporated to corroborate the results observed during these experiments and gave results which mimicked the experimental data.

015 – Development of ARL's Multi-Energy Flash Computed Tomography Diagnostic: Capability to Track Mass-Flux Through a Reconstruction Volume

Michael B. Zellner, Melissa S. Love, and Kyle Champley

The U.S. Army Research Laboratory and Lawrence Livermore National Laboratory are currently developing a Multi-Energy Flash Computed Tomography (MEFCT) diagnostic for multi-frame, in situ, three-dimensional radiographic assessment of ballistic impact phenomena. To accomplish this, we combine the capabilities of medical X-ray computed tomography and high-speed computed tomography, to produce a system that captures three independent, time-sequenced volume reconstructions throughout the timespan of a typical dynamic ballistic event. Because this system has the capability to image an event across three spatial dimensions and time, it is the first of its kind to track mass/material-flux of an un-bounded system through a volume at ballistic timescales. To demonstrate the diagnostic's capabilities, an assessment of a bullet penetrating an aluminum plate is performed. A compilation of the three volume reconstructions were computed to describe the event. The results were compared to a state-of-the-art simulation of the event using EPIC, a Lagrangian hydrocode with penetration applications. This comparison shows how using a four-dimensional computed tomography system can benefit the validation of physical failure and mass/material-flow models.

035 – Four-View Split-Image Fragment Tracking in Hypervelocity Impact Experiments

Erkai Watson, Nico Kunert, Robin Putzar, Hans-Gerd Maas, and Stefan Hiermaier

Fragmentation is a significant phenomenon caused by hypervelocity impact and has applications in orbital debris and planetary impact research, among many others. In particular, the velocity distribution of fragments created by hypervelocity impact is not thoroughly understood. In this paper, we present an experimental setup and analysis method for tracking and measuring individual fragment velocities in 3D. The setup uses two synchronized high-speed cameras with split images, yielding four views, to record image sequences of the in-flight fragments. We analyze the image sequences by identifying fragments and their trajectories in each view, matching the fragments found in different views, and finally triangulating for their 3D positions. The result is a method able to measure fragments' 3D velocities in the highly transient hypervelocity process.

112 – X-ray Diffraction Diagnostic Paired with Gas Gun Driven Compression of Polyethylene

Rachel C. Huber, Erik B. Watkins, Dana M. Dattelbaum, and Richard L. Gustavsen

Understanding the kinetics of phase transition and decomposition during extreme condition events is not a trivial undertaking. Capturing these processes require: 1) diagnostics that probe at energies capable of interacting with the dynamically evolving products, penetrating the opaqueness of the changing system; and 2) detectors sensitive enough to observe these events. Generation III Light Sources provides the access to a KeV x-ray beam capable of penetrating the opaque cloud with a wavelength adept at interacting with the evolved or compressed crystal structures. At the Dynamic Compression Sector at the Advanced Photon Source, gas guns produce planar shocks at a myriad of projectile velocities while capturing in situ x-ray diffraction of the evolving material under dynamic compression. Specifically we shocked high density polyethylene to 7.23 GPa observing compression of the polymer chains.

077 – Hypervelocity Sequenced Laser Shadowgraph Instrument and Measurement Of Debris Cloud With Hypervelocity

Ke Fawei, Huang Jie, Song Qiang, Wen Xuezhong, Li Xin, Xie Aimin, Li Jing, Jiang Lin, and Liu Sen

The hypervelocity sequenced laser shadowgraph instrument has been developed in China Aerodynamics Research and Development Center (CARDC) to obtain the clear images for

the transient process of hypervelocity impact, which has the characteristics of high definition ability of the time and the space, by solving the pessimistic influence of the intense flame in the measurement area. The shadowgraph instrument has the following three characteristics. Firstly, the image frame frequency and the image resolution are decoupled, i.e. the constant resolution of image is bigger than 10,000,000 pixels when the image interval is 10 ns. Secondly, the intense flame in the measurement area is eliminated, and the clear images of debris cloud with hypervelocity are obtained. Thirdly, image scale is same, i.e. the image can be used to measure the moving velocity of the debris cloud contour. The hypervelocity sequenced laser shadowgraph instrument is used to measure the debris cloud produced by Al sphere impacting the Al plate with velocities from 3.0 km/s to 8.3 km/s, and all clear images are obtained. The moving trajectories of debris cloud are obtained according to the calibration and processing image of the shadowgraph images. The measurement results showed that the developed shadowgraph instrument could be used to measure the debris cloud quantificationally.

024* – Simulating Lateral Drift of a Shaped Charge Jet in ALEGRA

Matthew J. Coppinger, W. Casey Uhlig, and John H. J. Niederhaus

This report investigates the ability of the shock Multiphysics hydrocode, ALEGRA, to simulate the lateral drift of a shaped charge jet through stochastic variations of simulation parameters. Stochastic variations in the explosive density and the liner initial yield strength, fracture pressure, and density were introduced, and a method was developed to compare the magnitude of lateral drift between the simulations. The extent to which each of the material parameter variations affected lateral drift is presented and compared to a baseline simulation. Variations in liner yield strength, liner fracture pressure, and explosive density were found to impart a modest amount of lateral drift, while variations in the liner density imparted a significant amount of lateral drift.

Technical Session 4:

Spacecraft Meteoroid and Debris Shielding I

(*denotes Poster Session)

048 – Investigation on Response of an Aluminum Honeycomb Subjected to Hypervelocity Impacts using Lagrange and SPH for Numerical Modeling

Kumi Nitta, Masumi Higashide, Mirai Sueki, and Atushi Takeba

Numerical modeling has been conducted with commercial code AUTODYN 2D, using Lagrange and Smooth Particle Hydrodynamics (SPH) processors. The numerical results are compared and discussed with the corresponding experimental results from the standpoint of assessing the protection of satellites against M/OD hypervelocity impacts. The material models used in the numerical simulation are also discussed, as well as a wide range of impact velocities, including shock-induced vaporization. The projectiles used to simulate M/OD consist of 100 μm to 1 mm of alumina with impact velocities of 2–15 km/s. In order to assess the structural integrity of unmanned spacecraft subjected to the threat of hypervelocity impact by space debris, the numerical method was proposed mainly from the standpoint of material modeling suitable for extremely severe physical conditions such as high pressure, high temperature, high strain, and a high strain rate, sometimes accompanied by shock-induced vaporization. The numerical results adopting these material models were compared with the corresponding hypervelocity impact tests by using the two-stage light-gas gun at ISAS/JAXA. Although examples of the impacts on the aluminum honeycomb can be shown, it has been demonstrated that the numerical analysis can effectively simulate the overall corresponding experimental results. We show the response of an aluminum honeycomb as derived from analysis of hypervelocity impact at 2 km/s to 15 km/s using Lagrange and SPH processors. We also verified that the ballistic limit curve of an aluminum honeycomb panel is shown as a downward line using both processors, which is unlike the up and down ballistic limit curve of a Whipple shield.

099 – Explosion of Hydrazine Tanks Due to Space Debris Impacts

Jérôme Limido, Christian Puillet, and Jean-Paul Vila

The impact of space debris on a spacecraft can result in a catastrophic event that not only destroys the structure but can also create more space debris. The design of any spacecraft requires understanding the potential damage that can be inflicted by such an event. Consider the case of a satellite hydrazine fuel tank and what happens as the result of a hypervelocity impact from space debris. The purpose of this study is to better understand the mechanisms of detonation of hydrazine vapor during a hypervelocity impact on a low-pressure reservoir. The IMPETUS Afea Solver® and Explo5 software were used to perform numerical simulations of operational impact configurations (v = 14km / s). The multi-scale calculations are performed using the Next Generation IMPETUS SPH solver. A numerical assessment of the impact performance at the scale of the reactive fluid reservoir representative of a real configuration (global and local scale) was carried out. The model includes the detonation in the fluid and the transfer of the momentum to the structure which includes capturing the perforation of the structure that results from the explosive loading.

118 – Hypervelocity Impact of PrintCast A356/316L Composites

Lauren L. Poole, Manny Gonzales, Matthew R. French, William A. Yarberry III, and Zachary C. Cordero

Shielding elements used to protect against micrometeoroids and orbital debris (MMOD) (e.g., Whipple shields, multi-shock shields, stuffed Whipple shields) typically incorporate thin bumper sheets that intercept and vaporize incident MMOD traveling at speeds in excess of several km/s. In some applications, however, space limitations prevent the use of large stand-offs, and components must instead be protected by a single monolithic shielding element. Electronics, for example, are often only protected by their housing. With such applications in mind, we describe a class of spatially efficient composite shielding elements fabricated using a hybrid additive manufacturing approach termed PrintCasting. The PrintCast process consists of two steps: First selective laser melting is used to fabricate a lattice preform in the shape of the final component. Next this preform is infiltrated with a liquid metal that has a melting point lower than that of the lattice. The resulting solidified part is a periodic interpenetrating composite in which each constituent forms a continuous network. Using a combination of hypervelocity impact experiments and shock transmission calculations, we demonstrate that these interpenetrating composite shielding elements mitigate spallation and other failure modes through multiple internal shock reflections at the buried heterophase interfaces.

066 – Using the DebriSat Fragments to Update the NASA Standard Satellite Breakup Model and Shape Effects on Ballistic Limit Equations

Heather Cowardin, Phillip Anz-Meador, James Murray, J.-C. Liou, Eric Christiansen, Marlon Sorge, Norman Fitz-Coy, and Tom Huynh

Existing DOD and NASA satellite breakup models are based on a key laboratory test, the 1992 Satellite Orbital debris Characterization Impact Test (SOCIT), which has supported many applications and matched on-orbit events involving older satellite designs reasonably well over the years. To update and improve these models, the NASA Orbital Debris Program Office, in collaboration with the Air Force Space and Missile Systems Center, The Aerospace Corporation, and the University of Florida, conducted a hypervelocity impact test using a high-fidelity mock-up satellite, DebriSat, in controlled and instrumented laboratory conditions. DebriSat is representative of present-day LEO satellites, having been constructed with modern spacecraft materials and techniques. The DebriSat fragment ensemble provided a variety of shapes, bulk densities, and dimensions. Fragments down to 2 mm in size are being characterized by their physical and derived properties. A subset of fragments will be analyzed further in laboratory radar and optical facilities to update the existing radar-based NASA Size Estimation Model (SEM) and develop a comparable optical-based SEM. Thoroughly understanding size estimates from ground-based optical and radar sensors is one of the key parameters used in assessing the environment and the risks that debris present to operational spacecraft. The data will inform updates to the current NASA Standard Satellite Breakup Model (SSBM); which was formulated using laboratory and ground-based measurements of on-orbit fragmentation events to describe an average breakup for spacecraft and upper stage collisions and explosions. DebriSat will extend the laboratory data ensemble. The DebriSat shape and density categories provide a baseline for non-spherical projectile hypervelocity impact testing for damage assessment. The data from these tests, simulations, and analyses will be used to update the NASA Orbital Debris Engineering Model (ORDEM) with more realistic simulations of catastrophic fragmentation events for modern satellites and to assess the risk posed by the orbital debris environment. This paper provides an overview of the project, updates on the characterization process, and the NASA analysis status.

044 – Simulation Study of Non-Spherical, Graphite-Epoxy Projectiles

Joshua E. Miller

The DebriSat hypervelocity impact experiment, performed at the Arnold Engineering Development Center, is intended to update the catastrophic break-up models for modern satellites. To this end, the DebrisSat was built with many modern materials including structural panels of carbon-fiber, reinforced-polymer (CFRP). Subsequent to the experiment, fragments of the DebrisSat have been extracted from porous, catcher panels used to gather the debris from the impact event. Thus far, one of the key observations from the collected fragments is that CFRP represents a large fraction of the fragments and that these fragments tend to be thin, flake-like structures or long, needle-like structures; whereas, debris with nearly equal dimensions is less prevalent. As current ballistic limit models

are all developed based upon spherical impacting particles, the experiment has pointed to a missing component in the current approach that must be considered. To begin to understand the implications of this observation, simulations have been performed using cylindrical structures at a representative orbital speed into an externally-insulated, double-wall shield that is representative of shielding on the current International Space Station crew transport vehicle, the Soyuz. These simulations have been performed for normal impacts to the surface with three different impact angles-of-attack to capture the effect on the shield performance. This paper documents the simulated shield and the models developed to study the effect of fragments and derives the critical characteristics of CFRP impacting particles for the selected shield. To assist with the design of the updated debris models, this work summarizes the simulated results into a deployable form for evaluating the relative importance of fragment structures.

018* – Consequences of Micrometeoroid/ Orbital Debris Penetrations on the International Space Station

James L. Hyde , Eric L. Christansen, and Dana M. Lear

Risk from micrometeoroid and orbital debris (MMOD) impacts on space vehicles is often quantified in terms of the probability of no penetration (PNP). However, for large spacecraft, especially those with multiple compartments, a penetration may have a number of possible outcomes. The extent of the damage (diameter of hole, crack length or penetration depth), the location of the damage relative to critical equipment or crew, crew response, and even the time of day of the penetration are among the many factors that can affect the outcome. For the International Space Station (ISS), a Monte-Carlo style software code called Manned Spacecraft Crew Survivability (MSCSurv) is used to predict the probability of several outcomes of an MMOD penetration—broadly classified as loss of crew (LOC), crew evacuation (EVAC), loss of escape vehicle (LEV), and nominal end of mission (NEOM). By generating large numbers of MMOD impacts (typically in the hundreds of billions) and tracking the consequences, MSCSurv allows for the inclusion of a large number of parameters and models as well as enabling the consideration of uncertainties in these models and parameters. MSCSurv builds upon the results from NASA's Bumper software (which provides the probability of penetration and critical input data to MSCSurv) to allow analysts to estimate the probability of LOC, EVAC, LEV, and NEOM. This paper provides an overview of the methodology used by NASA to quantify LOC, EVAC, LEV, and NEOM with particular emphasis on describing in broad terms how MSCSurv works and its capabilities and most significant models.

019* – Investigation on Sustained Discharge of Satellite's Power Harness Due to Plasma from Space Debris Impact

Yuki Mando, Koji Tanaka, Takayuki Hirai, Shirou Kawakita, Masumi Higashide, Hirohisa Kurosaki, Sunao Hasegawa, and Kumi Nitta

Space debris is traveling at the velocity of 7-8 km/s in a low Earth orbit (LEO) and 3 km/s in a geostationary Earth orbit (GEO). The impact between space debris and spacecraft will be tremendous damage. In particular, particles with a diameter of less than 1mm have a risk to result in a permanent sustained discharge (PSD). The PSD may affect a satellite's power system. The effect on solar arrays has been well studied because they have a large area have been studied well, but the effect on the bundle of satellite's wire harness called power harness has not been clarified in spite that the power harness is usually exposed to space without protection. We conducted the hypervelocity impact experiments using a two-stage light gas gun. We investigated the risk resulting in the PSD from hypervelocity impacts of less than 1mm-sized particles. In addition, we compared two kinds of circuit configurations: a more realistic circuit configuration with internal resistance and a circuit configuration without it so as to investigate whether the internal resistance affects the PSD occurrence or not. The gun accelerated projectiles of stainless steel or aluminum oxide with a diameter from 0.3 to 1 mm up to 7.16 km/s. Targets used the three-layered power harness with the power condition simulated in typical satellites operated in LEO or GEO. As a result, 11 shots of 28 resulted in the PSD. With the more realistic circuit configuration, we could not confirm any results in the PSD. We found that the PSD is less likely to occur in a more realistic circuit configuration.

043* – Numerical Modeling of Impacts of Twisted-pair Data Cables

Joshua E. Miller

Data wire cable runs are a significant presence on the exterior of the International Space Station (ISS), and continued ISS mission support requires detailed assessment of cables due to micrometeoroid and orbit debris (MMOD) impact. These data wire cables are twisted-pair cables consisting of two 22 gauge stranded conductors inside a tight-fitting, braided-copper shield and jacket having a nominal outer diameter of 3.76 mm. The ISS engineering community has identified two loss-of-function mechanisms for these cables: open circuits due to severed conductors within the cable, and short circuits due to contact between conductors or grounded components. Previous work has documented a total of 97 impact experiments that have been performed into these cables to develop an empirical, statistical model for the failure of these cables in reliability studies; however, the experimental work leaves open the internal behaviors that contribute to the probabilistic findings. To address this shortcoming, numerical impact simulations have been performed to expand the understanding of the acquired dataset.

055* – Hypervelocity Impact Performance of 3D Printed Aluminum Panels

Bruce A. Davis, Richard A. Hagen, Robert J. McCandless, Eric L. Christiansen, and Dana M. Lear

NASA, JSC has been developing light-weight, multi-functional sandwich core for habitable structure over the last several years. Early development involved a metallic open cell foam core, which is heavier than comparable honeycomb-based structures when non-structural requirements for deep space environments (vacuum, micro-meteoroids/orbital debris, and radiation) have not been considered. Unfortunately, honeycomb structures with an ordered, open path through the thickness have served to channel the micrometeoroid or orbital debris into the pressure wall (instead of disassociating and decelerating). While the metallic foam core represents a notable improvement in this area, there is an overwhelming need to further reduce the weight of space vehicles; especially when deep space (beyond low earth orbit, or LEO) is considered. NASA, JSC is currently developing a multi-functional sandwich panel using additive machining (3D printing), this effort evaluated the material response of a limited amount of 3D printed aluminum panels under hypervelocity impact conditions. The four 3D printed aluminum panels provided for this effort consisted of three body centric cubic lattice structure core and one kelvin cell structure core. Each panel was impacted once with nominally the same impact conditions (0.34cm diameter aluminum sphere impacting at 6.8 km/s at 0 degrees to surface normal). All tests were impacted successfully, with the aforementioned impact conditions. Each of the test panels maintained their structural integrity from the hypervelocity impact event with no damage present on the back side of the panel for any of the tests. These tests and future tests will be used to enhance 3D printed structural panels in future developments.

058* – Extravehicular Activity Micrometeoroid and Orbital Debris Risk Assessment Methodology

Kevin D. Hoffman, James L. Hyde, Eric L. Christiansen, and Dana M. Lear

A well-known hazard associated with exposure to the space environment is the risk of vehicle failure due to an impact from a micrometeoroid and orbital debris (MMOD) particle. Among the vehicles of importance to NASA is the extravehicular mobility unit (EMU) "spacesuit" used while performing a US extravehicular activity (EVA). An EMU impact is of great concern as a large leak could prevent an astronaut from safely reaching the airlock in time resulting in a loss of life. For this reason, a risk assessment is provided to the EVA office at the Johnson Space Center (JSC) prior to certification of readiness for each US EVA.

Technical Session 5:

High Velocity Penetration and Target Response II

(*denotes Poster Session)

104 – High Velocity Impact Testing for Evaluation of Intermetallic Projectiles

Kevin J. Hill, Colt Cagle, Connor Woodruff, Michelle L. Pantoya , Joseph Abraham, and Casey Meakin

A High-velocity Impact-ignition Testing System (HITS) was developed to study the dynamic response of intermetallic projectiles penetrating through aluminum plates at speeds up to 1500 m/s. Experiments were performed to study penetration through multiple aluminum plates followed by impact into an inert steel anvil. The intermetallic projectiles are pellets contained in a .410 caliber shot gun shell and launched from a propellant driven gun into a catch chamber equipped with view ports and imaging diagnostics. The penetration, impact and reaction events are monitored using high-speed cameras that provide a local and macroscopic perspective of impact and subsequent reactions. Results demonstrate the range of visual data that can be captured by a non-gas generating intermetallic charge that fragments and reacts upon penetration and impact. Results show that higher velocity projectiles (~ 1300 m/s) produce smaller fragments upon penetration that result in flame spreading through the chamber while lower velocity projectiles (~ 500 m/s) exhibit larger fragments that produce no flames.

014 – Towards a Better Understanding of Shaped Charge Jet Formation and Penetration

David W. Price, Ernest J. Harris, and Frances G. Daykin

JeMMA, a set of relatively simple shaped-charge devices, has been designed in order to generate suitable data on jet formation, break-up and penetration for code validation

purposes. The JeMMA Phase 1 device incorporated a copper liner and six of these shaped charges were manufactured as a technology demonstrator by SAAB Bofors Dynamics Switzerland Ltd and fired in their shaped charge facility in Switzerland in December 2016. The radiographic results obtained from the JeMMA Phase 1 and 2 devices, along with data reproducibility between trials, was excellent. This report gives an overview of the Phase 1 and 2 trials, including device design, the results of the firings conducted in Switzerland and details of the subsequent 2D and 3D hydrocode modelling carried out at AWE. The agreement between the data and both 2D and 3D modelling of the experiments is very pleasing, but highlights where further work is required. These JeMMA experiments will enhance the body of relevant data required to provide the validation of the hydrocode materials and modelling methodologies and enable us to better model the jetting threats of our experiments and have higher confidence in the results of the modelling.

036 – Prediction of Micrometeoroid Damage to Lunar Construction Materials using Numerical Modeling of Hypervelocity Impact Events

Maria I. Allende, Joshua E. Miller, B. Alan Davis, Eric L. Christiansen, Michael D. Lepech, and David J. Loftus

The use of Lunar regolith for the creation of construction materials to build habitats and other Lunar base infrastructure is an example of in situ resource utilization, an important strategy to minimize a NASA mission's launch mass by leveraging materials found at an exploration destination. One class of solidified regolith, Biopolymer-bound Soil Composites (BSC), consists of regolith mixed with a small amount of biopolymer binding agent (10% w/w). This paper characterizes BSC's micrometeoroid impact performance using experimental and numerical methods. Micrometeoroids are a notable hazard of the lunar environment and pose a challenging design consideration. A total of 17 hypervelocity impact experiments were conducted on BSC targets at NASA's White Sands Testing Facility. Numerical simulations of the hypervelocity impact experiments were carried out using CTH, a shock physics code developed by Sandia National Laboratories. Comparisons between the experimental craters and the simulation results indicate that there is good agreement between crater dimensions of the hypervelocity impact experiments and the CTH model. The CTH model developed in this paper provides (1) a damage prediction tool that allows for the necessary extrapolation of micrometeoroid impact velocities beyond what is experimentally achievable and into the velocity regime that is relevant for micrometeoroids and (2) a material design tool that is capable of varying material parameters computationally, ultimately allowing for the engineering and optimization of BSC's performance under impact loading.

119 – A Predictive Non-Dimensional Scaling Law for the Plate Perforation of Several Aluminum Alloys by Fragment-Simulating Projectiles

Weinong Chen and Zherui Guo

An equation was previously-presented to predict the ballistic-limit velocity for the perforation of aluminum armor plates by fragment-simulating projectiles (FSP). The ballistic-limit equation was presented in terms of dimensionless parameters so that the geometric and material problem scales are identified. Previously published predictions and data for two different FSP projectile calibers (12.7 mm and 20 mm) and two different strength aluminum alloys show the scaling law to be accurate. In this paper we extend the same concept to several other alloys and show that this scaling law is predictive.

063 – Modeling Hypervelocity Impact of Reinforced Carbon-Carbon Composite Thermal Protection System

Alexander J. Carpenter, Sidney Chocron, and James D. Walker

Reinforced carbon-carbon (RCC) composite is used in applications where structural stiffness and strength must be maintained at very high temperatures that may reach 2000°C or more. For example, it was used on both the Space Shuttle's nose cone and the leading edges of its wings. As exemplified by the Space Shuttle Columbia accident, the ability of these materials to survive impacts up to hypervelocity speeds can be critical for some applications. As computational modeling becomes an increasingly important component of the design process, the ability to accurately model RCC materials under impact conditions likewise becomes more and more important. This paper describes a computational model of the thermal protection used on the Space Shuttle orbiter. The model incorporates both the RCC comprising much of the protection system and its silicon carbide coating. The model was subjected to hypervelocity impacts with both steel and aluminum projectiles, and the results were compared to test data from the literature.

023 – Dynamic Fragmentation of Boron Carbide with Laser-Driven Impact

Debjoy D. Mallick and KT Ramesh

Laser-driven micro-flyer plates exhibit high planarity within the first 500 microns of travel, but deform into curved impactors due to loss of flight-driving plasma at the edges of the plate and interaction of the plate with the atmosphere [1]. This time-of-flight based tunability of impactor geometry potentially offers adjustable loading conditions in stress space. Here we explore the dynamic fracture of Boron Carbide under loading at 1100-1200m/s impact velocities (strain rates of 106 s-1) from two impactor geometries: (1) a flat Al micro-flyer and (2) an Al micro-flyer with a radius of curvature. We compare these results to prior ballistic experiments with a spherical projectile impacting at 930m/s. In-situ high-speed imaging at 10 million frames-per-second allows us to characterize the flyer geometry and identify active failure mechanisms in the target. Photon Doppler Velocimetry provides the target free surface velocity history and allows estimates of the internal stress state during failure. Optical microscopy of generated fragments link the microstructure to fragmentation behavior.

Technical Session 6:

Armor/Anti-Armor and Ballistic Technology

(*denotes Poster Session)

093 – Effect of Liquid Parameters on Protective Performance of Liquid Composite Target Subjected to Jet

Tan Yaping, Jia Xin, Huang Zhengxiang, Cai Youer, and Zu Xudong

In order to study the influence of liquid parameters on the protective performance of liquid composite targets (LCT), based on the theory of interaction between jet and LCT, three dimensionless numbers C, G and V are obtained by dimensional analysis in this paper. These 3 dimensionless numbers represent the compressibility, inertia and viscosity of liquid, respectively. The empirical formula, , was obtained by fitting the experimental data of static depth of penetration (DOP) experiment which can predict the residual depth of penetration(RDOP) of jet penetrated the LCT. It turns out that the 2 dimensionless C and G, which characterize the compressibility and inertia of liquid, play a decisive role in in the protection performance of LCT, while the influence of liquid viscosity is small. In addition, according to the research results of this paper, the protective performance of LCT can be improved by selecting liquid with high sound velocity, high viscosity and low density.

050 – Defeating Modern Armor and Protection Systems

Markus Graswald, Raphael Gutser, Jakob Breiner, Florian Grabner, and Timo Lehmann

An open source research and vulnerability study of main battle tanks and their protections systems revealed that current anti-tank weapons may not be suited to defeat modern threats. One example is the novel T-14 tank being developed and tested in the Russian army with its combined hard-kill and soft-kill active protection system AFGANIT / SHTORA, its new reactive armor MALACHIT as well as improved multi-component passive armor. Additionally, modern active protection systems currently developed in, e.g., Israel, the United States, and Germany feature also multi-sensor and multi-effector systems with drastically improved detection and intercept ranges, short system reaction times as well as protection against multiple threats attacking simultaneously and / or from similar directions. While known effectors and concepts may overcome fielded active protections systems, they are probably not suited in defeating such modern and even future systems. Countermeasures relying on high engagement velocities through improved kinetic energy projectiles or hypervelocity penetrators may provide a potential solution. Another promising concept generates directed, far-distance electromagnetic effects defeating sensors and communications systems of modern main battle tanks. After such a mission kill, a following salvo attack through an anti-tank or modern multi-role weapon will eventually lead to a catastrophic kill. Feasibility studies of these mobile electromagnetic effectors have already shown their high potential.

110 – 3D Printed Conical Shaped Charge Performance

Phillip Mulligan, Catherine Johnson, Jason Ho, Cody Lough, and Edward Kinzel

A conical shaped charge is a versatile device utilized in both the petroleum and defense industries. The geometry and material structure of the metal cone play an integral role in the conical shaped charge performance. The performance of conical shaped charge liners has been relatively well-characterized for liners manufactured via hydroforming, hydraulic pressing, on a lathe, or using Computer Numerical Controlled (CNC) machines. With advancements in additive manufacturing conical shaped charge liners can be 3-Dimensionally (3D) printed with metal powders. However, it is unclear as to how 3D printing the metal liners, with Selective Laser Melting (SLM), will influence the conical shaped charge's performance. This paper explores the performance, relative to penetration, of conical shaped charges with 3D printed metal liners. While most conical shaped charges that do not utilize pressed metals

for the liners utilize cold or hot rolled copper, formed into the liner geometry, due to copper's high ductility. However, 3D print material limitations required all the liners be made from 304 stainless steel. The metal liners were printed with the highest melt density achievable with the University's SLM printer. The metal liner dimensions (thickness, height, and outer diameter) were designed using the recommended ratios of the liner's inner diameter presented by Virgil (1988). The 3D printed metal liners are compared to a CNC machined liner, with the same dimensions. The comparison enables the evaluation of how 3D printing a liner influences penetration performance. The results indicate conical shaped charges could utilize 3D printed liners. These results open a wide range of performance design opportunities that cannot be achieved via conventional manufacturing and justify the current increased cost associated with additive manufacturing metal components. Future work will continue to explore how print density, printed material, and advanced geometries modify the conical shaped charge performance.

004 – Calculation of Jet Characteristics from Hydrocode Analysis

Justin C. Sweitzer, Scott D. Hill, and Nicholas R. Peterson

The penetration performance of a shaped charge jet is affected strongly by factors such as straightness, stretch rate, and breakup time. Straightness is related to manufacturing tolerances, assembly techniques, and system integration features. Stretch rate and breakup time are controllable features of charge design. A higher stretch rate is desirable for short standoff performance. The stretch rate is easily altered by a change of explosive or modification of the angle with which the detonation wave sweeps the liner surface, however, an increased stretch rate generally results in a decreased breakup time. Many of the recent gains in shaped charge performance have been made possible by increasing the effective breakup time of the jet. Several models exist for calculating breakup time. They include analytic models, such as Chou & Carleone's dimensionless strain rate model, and empirical or semi-empirical models such as Walsh's theory and those proposed by Pearson, et al. These models can be applied to raw hydrocode calculation data and used to determine a Jet Characterization (JC) file. The JC file can then be used to perform further calculations, such as Penetration Versus Stand Off (PVSO) curves. This paper details adaptation of the Chou & Carleone model for predicting breakup time using hydrocode data. The hydrocode is used to determine the physical parameters of the jet which are then extrapolated back to a virtual origin for breakup time calculation. This results in a model that is design independent, relying on hydrocode determination of jet variables. The model implementation will be discussed, and comparisons of predicted jet characteristics will be made to test data for several charge geometries.

003* – Analysis of the Distribution of BAD Generated During the Normal Penetration of Variable Cross-Section EFP on RHA

Boyang Xing, Yunhui Hou, Zhenyan Guo, Dongjiang Zhang, Liang Chen, Yongliang Yang, Jianhua Luo, Rongzhong Liu, and Rui Guo

This paper purposes to analyze how the thickness of Rolled Homogeneous Armor (RHA) and the impact velocity of Explosively Formed Projectile (EFP) influence the number of middle mass behind-armor debris (BAD) when variable cross-section EFP penetrates RHA normally. The numerical simulation is adopted, the thickness of RHA is from 10mm to 70mm, the impact velocity of EFP is from 1650m/s to 1860m/s. The results indicate that: (1) As the impact velocity of EFP is 1650m/s and the thickness of RHA is from 10mm to 70mm, p1g of RHA and EFP is decreasing with the increase of H0. And the thin target could be used to produce a large proportion of middle mass BAD from RHA (including BAD from EFP, BAD from RHA and EFP). (2) As the impact velocity of EFP is from 1650m/s to 1860m/s and the thickness of RHA is 40mm, p1g of RHA is less than 50%, p1g of EFP is more than 70%, p1g of RHA and EFP is more than 50%.

069* – Evaluation of Critical Ricochet Angles for 25mm APDS-T Projectile on Metallic Targets - Modeling and Verification

Alon Weiss, Asaf Borenstein, Vitaly Paris, Moshe Ravid, and Nimrod Shapira

This paper is a study on ricochet characteristics of metal plates hit by 25 mm APDS-T projectile. A series of ballistic tests has been carried out on three different armor steel types chosen to present a range of hardness. Each armor steel target was impacted at varying angles of incidence until ricochet was observed. This investigation is not only expected to help in understanding the phenomenon of projectile ricochet but also to provide some useful data that can be used for calibration and validation of the finite element (FE) models. In general, the ricochet angle was found to decrease with an increase in target hardness due to different failure mechanism.

094* – Effects of Additional Body on Jet Velocity of Hyper-cumulation

Xu Mengwen, Jia Xin, and Huang Zhengxiang

In this paper the effects of the additional body's material, thickness and diameter on the velocity with different cone angles of the liner is studied by AUTODYN-2D. The results show as follows: 1. From the top of the liner to the end, the additional body can increase the top velocity of the jet formed by the hyper-cumulation, but have little effect on the tail velocity. 2. When the cone angle is different, the changes of the head velocity are in the similar laws. The larger the cone angle, the more increases of it, which is about 36%. As well as the greater the velocity gradient of jet head. 3. The increase of jet head velocity by additional body is independent of material yield strength but has the greatest correlation with density. Different materials of additional body have the same region for increasing jet velocity. With the increase of material density, the velocity gradient of the jet head increases, and the finer the jet head is formed. 4. The larger the density of the additional body is, the smaller the optimum thickness is. When the thickness is not less than the optimum thickness, increasing the diameter of the additional device can improve the velocity of the jet head and the stability of the jet forming process, so that the jet is not easy to break up. Consequently, it is proposed that this kind of hyper-cumulation structure, with a flat plate additional body, is more suitable to improve the classical liner with large cone angle. By improving the structure in this way, the velocity, mass and breaking time of the jet formed by the liner can be increased, so that the penetration power will be enhanced compared with the classical one. 100* - Study on jet formation and penetration of double layer explosive sub-caliber shaped charge, Yu-ting Wang.

100* – Study on Jet Formation and Penetration of Double Layer Explosive Sub-caliber Shaped Charge

Yu-ting Wang, Qiang-qiang Xiao, Zheng-xiang Huang, Xu-dong Zu, and Bin Ma

The traditional shaped charge can hardly reach the kill-radius index because of its structure, In order to adapt to the different battlefield, this paper proposed a new shaped charge with insensitive explosive appended to its outer layer, called double layer explosive sub-caliber shaped charge. In this paper, conduct the Ø56 mm shaped charge as benchmark shaped charge. The simulations were carried out by AUTODYN for jet formation and penetration of different axial thickness of the additional insensitive explosive and the additional height of charge, with the aim to obtain the optimal size of double-layer explosive sub-caliber shaped charge. The results show that the optimum axial thickness of the additional insensitive explosive is $\Delta R / R_0 = 0.8$, the optimum size of additional height of charge is $\Delta L / L_0 = 0.4$.

125* – Effects of Stacking Order on the High-Velocity Impact Response of Bi-Material Soft Armor Systems

Zherui Guo, Stephenie Martinez-Morales, and Weinong W. Chen

The impact response of mono-material soft armor fabric targets has been shown to be diphasic and decoupled at their ballistic limit velocity. This diphasic response is not sustained with increasing impact velocities past the ballistic limit velocity for a given target. At these velocity regimes, the impact response of the target is shown to be monophasic. In such cases, the selection criteria of the materials and the stacking order may play a different role than at ballistic limit velocities. The effects of stacking order of a bi-material target panel are investigated across a range of striking velocities at and past the ballistic limit. The base soft armor being investigated is Twaron® CT709, while secondary panel materials chosen are polyurea and Dyneema® SB31 panels extracted from existing vests. Mass ratios of primary and secondary materials in a single armor are approximately 50/50 respectively. Panels are tested with the primary Twaron® fabric at the strike face and the rear face to determine the evolution of ballistic limit velocity, energy-absorption mechanisms, and failure modes.

Technical Session 7:
Fracture and Fragmentation

(*denotes Poster Session)

061 – Assessment and Validation of Collision "Consequence" Method of Assessing Orbital Regime Risk Posed by Potential Satellite Conjunctions

Travis F. Lechtenberg and Matthew D. Hejduk

Collision risk management theory requires a thorough assessment of both the likelihood and consequence of potential collision events. Satellite conjunction risk assessment has produced a highly-developed theory for assessing the likelihood of collision but typically neglects to account for the consequences of a given collision. While any collision may compromise the operational survival of a space-craft, the amount of debris produced by the potential collision, and therefore the degree to which the orbital corridor may be compromised, can vary greatly among satellite conjunctions.

Previous studies leveraged work on satellite collision modeling to develop a method to estimate whether a particular collision is likely to produce a relatively large or relatively small amount of resultant debris. The approximation of the number of debris pieces is dependent on a mass estimation process for the secondary objects utilizing the radar cross section of said object. This study examines the validity of the mass estimation process and establishes uncertainty bounds on the secondary object mass which will be used to best approximate the possible consequences of a prospective collision. This process is then applied to a large set of historical conjunctions to assess the frequency at which possible collisions may significantly augment the orbital debris environment in operational spacecraft.

097 – Characterization of the Ballistic Properties of Ejecta from Laser Shock-Loaded Samples Using High Resolution ps Laser Imaging

Arnaud Sollier and Emilien Lescoute

A high resolution ps laser imaging diagnostic has been developed for making high-resolution spatial measurements of ejecta particles moving at high velocities (a few km/s). Preliminary results obtained with both visible (532 nm) and UV (355nm) lighting are presented for laser shock-driven tin ejecta experiments performed with different kind of surface defaults. These results are compared with those obtained at LANL under high explosive loading using ultraviolet in-line Fraunhofer holography, and also with molecular dynamics (MD) simulations performed at lower space and time scales.

120 – Conical Impact Fragmentation Test (CIFT)

Christopher Neel, Peter Sable, Philip Flater, and David Lacina

AFRL/RW conducted experiments to develop an experimental capability for uniformly and controllably inducing fragmentation in structural metals. The setup involves a conical specimen impacting a mating conical target (similar in geometry to a funnel) at nominal velocities of 1 - 2 km/s. Three experiments were conducted as proof of concept to characterize the fragmentation behavior of 1018 steel. PDV probes on the free outer surface of the cone allow for validating simulations that can indicate strain uniformity in the target cone. Overall, experimental results demonstrate the conical impact fragmentation test (CIFT) to be a feasible method by which to evaluate fragmentation behavior. The conical geometry produces consistent and bounded strain rates that are maintained for at least 10 microseconds. Furthermore, when compared with other laboratory techniques, the CIFT technique is shown to be either more ideal (when compared to sphere-on-plate impact, SPI) or more tunable (when compared with cylinder expansion, CYLEX) and so is a promising fragmentation characterization tool.

022 – Bulking as a Mechanism in the Failure of Advanced Ceramicss

Brendan M. L. Koch, Calvin Lo, Tomoko Sano, and James David Hogan

Failure in brittle materials is characterized by crack growth and fracture, processes which involve an increase in the volume of a sample to accommodate these cracks. This process is called bulking and it is known to be an important factor in the failure of materials such as ceramics, stone, and concrete. While volumetric strains are obtainable under quasi-static conditions, under dynamic conditions technical challenges have stood in the way of obtaining multi-dimensional strain data that would allow for assessment of bulking under the sort loading conditions that would simulate a high velocity impact. Advances in digital-image-correlation and ultra-high-speed-photography have however opened up the capacity to obtain this higher dimensional data. This data in turn has prompted an assessment of prior theory to produce a framework through which stress-strain behavior can be expressed in terms of changes to multiple elastic constants simultaneously. This presentation offers initial results in quasi-static and dynamic experiments and discusses the implications for brittle material behavior and crack evolution phenomenon under a variety of conditions.

056 – The Role of Inclusions in the Failure of Boron Carbide Subjected to Impact Loading

Andrew L. Tonge and Brian E. Schuster

This work investigates the importance of the microstructure of boron carbide for initiating inelastic deformation under impact conditions. Simple loading resulting from a flyer plate impact geometry is used to illustrate the importance of microstructure for the well-controlled and easily instrumented experimental geometry. A second set of simulations is performed on a miniaturized impact geometry to investigate the importance of the microstructure for the early stages of semi-infinite penetration for impact velocities between 0.9 km/s and 1.9 km/s. The effect of the microstructure is more pronounced for the flyer plate impact geometry.

089 – Pagosa Simulation of Hypervelocity Impact and Fragmentation from Hypersonic Explosions

Xia Ma, David Culp, and Brandon Smith

We use PAGOSA's FLIP+MPM capability to simulate hypervelocity impact and fragmentation from hypersonic explosions. The scenario to be simulated involves a complex chain explosion from fragmentation impact which was caused by another explosion. The simulations also use the SURF model for shock to detonation transition (SDT) and the MATCH model for mechanical ignition and deflagration of high explosives. These models in PAGOSA working together are crucial for modeling complex system for real world applications. This shows the powerful modeling and predicting capability of PAGOSA that others cannot do. Since experimental data are not available for any complex scenario like this, we did verification and validation (V&V) in each separate steps. These include the fragmentation simulated by FLIP+MPM, the Shock to Detonation Transition (SDT) modeled by SURF and mechanical ignition and deflagration modeled by MATCH. PAGOSA is a shock hydrodynamics program developed at Los Alamos National Laboratory (LANL) for the study of high-speed compressible flow and high-rate material deformation. PAGOSA is a three-dimensional Eulerian finite difference code, solving problems with a wide variety of equations of state (EOSs), material strength, and explosive modeling options. It has high efficiency for simulations running on massively parallel supercomputers. It is a multi-material code using volume of fluid (VOF) interface reconstruction and second order fully explicit time integration. Standard von Neumann artificial viscosity is used. Newly added material point method (MPM) plus Fluid-Implicit Particle (FLIP) capability can simulate high-speed metal fragmentation.

025 – Deformation and Acceleration of Zn and Cu Liners Under Explosive Shock Loading

Puwadet Sutipanya, Fumikazu Saito, Mitsuyori Nakashita, Takashi Ogino, Yutaka Takizawa, Yohsuke Okada, and Masahiko Natsubori

Both zinc and copper shaped charge jets (SCJs) generated from conical liners under explosive shock loading were observed using soft flash X-ray radiography. The goal was to ascertain the effect of the liner material melting point on the jet features and density. An analytical method termed in situ mass analysis from X-ray image processing (i-MAX) was utilized to estimate the mass and apparent density of each SCJ in this study. The masses determined for the zinc and copper leading jets were (34 ± 2) mg and (68 ± 3) mg, respectively. The overall mass distributions of both the zinc and copper SCJs showed the same tendency to decrease toward the tip of the jet, with the exception of the leading jet. The density distribution of the zinc SCJ gradually decreased toward the leading jet as it stretched. In contrast, the density distribution of the copper SCJ varied depending on the appearance of a necking region, and the minimum apparent density was observed 30 mm from the leading jet. These results demonstrate that the occurring of both cavitation and a dynamic vacancy (which affect the density distribution of the metal jet) depend on the melting point of the liner material.

041* – Modelling the Fracture of High-Hardness Armour Steel in Taylor Rod-on-Anvil Experiments

Brodie McDonald, Shannon Ryan, Nathan Edwards, Nikki Scott, Rory Bigger, Sidney Chocron, and Adrian Orifici

threshold of a high hardness armour steel (HHA) obtained through explicit finite element simulations. Using a stress triaxiality and Lode angle dependent failure strain criterion (Basaran 3D fracture locus), the constants for which were determined from quasi-static mechanical characterisation tests, the simulations were unable to predict the onset of fracture observed in the experiments. The rods exhibited principal shear failure under negative stress triaxialities, a condition that can be closely linked to adiabatic shear band (ASB) formation. As such, a strength fading criterion is proposed using a phenomenological description to capture the loss of load-carrying capacity resulting from ASB formation. The ASB criterion is based on an exponential fit to experimentally-observed instability strains measured at different average stress triaxialities in a series of tests on inclined cylindrical and modified flat-hat specimens. With the prediction of ASB formation the material strength is reduced to model the thermal softening experienced in the shear band, and fracture of the material (in the form of element erosion) remains controlled by the Basaran fracture model. Incorporating the ASB-based criterion, the numerical models were found to accurately predict both the impact velocity fracture threshold, as well as the general appearance of the observed principal shear fracture. The proposed criterion enables the effects of ASB formation to be captured in an impact simulation with little increase in computational cost.

051* – Shear Band Characteristics in High Strain Rate Naval Applications
Michael J. P. Conway, and James D. Hogan

This paper explores the dynamic behavior of HSLA 65 naval steels, specifically focusing on the initiation and growth of shear bands in quasi-static and dynamic compression experiments and how these bands affect stress-strain responses. The results indicate that the yield strength for this HSLA 65 increases from 541 ± 8 MPa for quasi-static (10-3 s-1) to 1081 ± 48 MPa for dynamic rates 1853 ± 31 s-1, and the hardening exponent increases from 0.376 ± 0.028 for quasi-static to 0.396 ± 0.006 for dynamic rates. Yield behavior was found to be associated with the onset of shear banding for both strain-rates, confirmed through visualization of the specimen surface using high-speed and ultra-high-speed cameras. For the quasi-static case, shear banding and yielding was observed to occur at 2.5% strain, and were observed to grow at speeds of upwards of 38 mm/s. For the dynamic experiments, the shear banding begins at approximately 1.18 ± 0.06% strain and these can grow upwards of 2122 ± 213 m/s during post-yield softening. Altogether, these measurements are some of the first of their kind in the open literature, and provide guidance on the critical time and length scales in shear banding. This information can be used in the future to design more failure-resistant steels, which has broader applications in construction, defense and natural resource industries.

085* – Modelling Fragmentation within Pagosa Using Particle Methods
David B. Culp and Xia Ma

The mechanics involved in shock physics often involves materials undergoing large deformations being subjected to high strain rates and temperature variations. When considering high-velocity impacts and explosions, metals experience plastic flow, dynamic failures and fragmentation that are often too complex for a Lagrangian method, such as the finite element method, to properly resolve. Conversely, Eulerian methods are simple to setup, but often result in numerical diffusion errors [1]. These unpleasantries can be skirted by using an alternative technique that incorporates a blend of these aforementioned methods. FLIP+MPM employs Lagrangian points to track state quantities associated with materials as strength, as well as conserved quantities, such as mass. Concurrently, an Eulerian grid is used to calculate gradient fields and incorporate an algorithm that carries out the hydrodynamics [2]. By incorporating the FLIP+MPM method into Los Alamos National Laboratory's Pagosa hydrodynamics code, massively parallel architectures may be employed to solve such problems as those including fragmentation, plastic flow and fluid-structure interaction. This paper will begin with a mathematical description of the FLIP+MPM technique and describe how it fits into Pagosa. After a description of the implementation, the capabilities of this numerical technique are highlighted by simulating fragmentation as a result of high velocity impacts and explosions. Several strength and damage models will be exercised to demonstrate the code's flexibility. Comparison of the different models' fragment size distributions are given and discussed.

Technical Session 8:
Analytical and Numerical Methodologies I
(*denotes Poster Session)

078 – An Accurate SPH Scheme For Hypervelocity Impact Modeling
Anthony Collé, Jérôme Limido, Thomas Unfer, and Jean-Paul Vila

We focus in this paper on the use of a meshless numerical method called Smooth Particle Hydrodynamics (SPH), to solve fragmentation issues as Hyper Velocity Impact (HVI). Contrary to classical grid-based methods, SPH does not need any opening criteria which makes it naturally well suited to handle material failure. Nevertheless, SPH schemes suffer from well-known instabilities questioning their accuracy and activating nonphysical processes as numerical fragmentation. Many stabilizing tools are available in the literature based for instance on dissipative terms, artificial repulsive forces, stress points or Particle Shifting Techniques (PST). However, they either raise conservation and consistency issues, or drastically increase the computation times. It limits then their effectiveness as well as their industrial application. To achieve robust and consistent stabilization, we propose an alternative scheme called γ-SPH-ALE. Firstly implemented to solve Monophasic Barotropic flows, it is secondly extended to the solid dynamics. Particularly, based on the ALE framework, its governing equations include advective terms allowing an arbitrary description of motion. Thus, in addition of accounting for a stabilizing low-Mach scheme, a PST is implemented through the arbitrary transport velocity field, the asset of ALE formulations. Through a nonlinear stability analysis, CFL-like conditions are formulated ensuring the scheme conservativity, robustness, stability and consistency. Besides, stability intervals are defined for the scheme parameters determining entirely the stability field. Its implementation on several test cases reveals particularly that the proposed scheme faithfully reproduces the strain localization in adiabatic shear bands, a precursor to failure. By preventing spurious oscillations in elastic waves and correcting the so-called tensile instability, it increases both stability and accuracy with respect to classical approaches.

090 – Analytically Derived Space Time-Based Boundary Condition (STBC) to Account for Stress Wave Propagation in Heterogeneous Micromechanical Model at Hypervelocity Impact
Zhiye Lia and Somnath Ghosh

The recent years have seen a surge in research on material and structural response of composites using homogenization based hierarchical modeling method. The microstructural representative volume element (RVE) is a small micro-region for which the volume average of variables is the same as those for the entire body. It is representations of the microstructure that is used for micromechanical simulations to determinate of effective material properties by homogenization. Conventionally, periodic boundary conditions (PBC) are applied on the RVE boundary. However, when the heterogeneous microstructure is under very high strain rate loading conditions (10^5 s^{-1} –10^7 s^{-1}), periodic boundary conditions (PBC) do not represent the accurate effect of stress wave propagation. Improper boundary conditions can lead to significant error in homogenized material properties. In order to increase the accuracy of the homogenization model, this study introduces a new space-time dependent boundary conditions (STBC) for 3D microscopic RVE subjected to high strain rate deformation in explicit FEM simulation by using characteristics method of traveling waves. The advantages of the STBC are discussed by comparing with time-dependent averaging results of examples using PBC. The proposed STBC offer significant advantages over conventional PBC in the RVE-based analysis of heterogeneous materials.

060 – Validation of an Improved Contact Method for Multi-Material Eulerian Hydrocodes in Three-Dimensions
Kenneth C. Walls and David L. Littlefield

Realistic and accurate modeling of contact for problems involving large deformations and severe distortions presents a host of computational challenges. Due to their natural description of surfaces, Lagrangian finite element methods are traditionally used for problems involving sliding contact. However, problems such as those involving ballistic penetrations, blast-structure interactions, and vehicular crash dynamics, can result in elements developing large aspect ratios, twisting, or even inverting. For this reason, Eulerian, and by extension Arbitrary Lagrangian-Eulerian (ALE), methods have become popular. However, additional complexities arise when these methods permit multiple materials to occupy a single finite element. Multi-material Eulerian formulations in computational structural mechanics are traditionally approached using mixed-element thermodynamic and constitutive models. These traditional approaches treat discontinuous pressure and stress fields that exist in elements with material interfaces by using a single approximated pressure and stress field. However, this approximation often has little basis in the physics taking place at the contact boundary and can easily lead to unphysical behavior. This work presents a significant departure from traditional Eulerian contact models by solving the conservation equations separately for each material and then imposing inequality constraints associated with contact to the solutions for each material with the appropriate tractions included. The advantages of this method have been demonstrated with several computational examples. This work concludes by drawing a comparison between the method put forth in this work and traditional treatment of multi-material contact in Eulerian methods.

111 – Higher-order Finite Elements for Lumped-Mass Explicit Modelling of High-Speed Impacts
Kent Danielson, Bob Browning, and Mark Adley

This paper describes the recent advances in higher-order finite elements for lumped-mass explicit approaches typically needed for high-rate impact modelling. Topics include benefits of 2nd order tetrahedral, wedge, hexahedral, and pyramid element formulations for both compressible and nearly incompressible materials as well as at higher orders, and effective explicit time solution methods. These 2nd order elements eliminate the need for hourglass control and provide higher resolution with fewer elements, since a single element can inherently capture curvature and flexural modes. 2nd order elements can also simplify meshing, since in contrast to certain types of 1st order elements, they are less prone to volumetric locking associated with near incompressibility, such as what occurs in metal plasticity; methods to avoid severe locking are available at the element level so as to permit unstructured meshing, e.g., typical all-tet methods or hexahedral-dominant methods. These technologies were developed within the U.S. Army Engineer

Research and Development Center-Geotechnical and Structures Laboratory (ERDC-GSL) in-house meshing (ProMesher), parallel analysis (ParaAble), and visualization (PenView) codes as well as placed into popular production software for meshing (Cubit), parallel analysis (EPIC), and visualization (ParaView). Examples using hexahedral-dominant meshes are provided, demonstrating the ability of an unstructured 2nd order model using all four element types to accurately simulate high-rate impact problems. The benefits for shape optimization and large tradespace analyses are also demonstrated.

091 – Multiscale Modeling of Reactive Structural Materials

Grant Smith, Scott Bardenhagen, and John Nairn

Material point method (MPM) simulations of model reactive structure materials (RSMs) have been performed at the mesoscale. The MPM methodology employed allows us to generate representative microstructures of RSMs comprised of highly-compacted powders of two or more metals. MPM simulations of the RSM microstructures under shock and tensile loading utilizing EOS and constitutive models for the component materials as well as advanced contact models for grain-grain interactions allows us to predict the mechanical and thermal behavior of the RSMs, including the role of particle-particle friction, as a function of RSM composition and loading scenario. The results of these extensive mesoscale simulations provide an extensive database of mechanical, thermal and failure behavior needed to derive homogenized EOS, constitutive and damage mechanics models for the RSMs. The homogenized models for the RSMs, which including advanced anisotropic mechanics models, can then be used in MPM simulations of the material in shock, impact and penetration scenarios at the engineering scale and allow prediction of RSM fragmentation.

053* – A Multi-Component Multi-Reaction Model for Aluminized Explosives

Shannon Lisenbee and David L. Littlefield

Traditional reactionary models for energetic materials generally fell into one of two camps: a single reaction model used for the decomposition of the energetic material or a separate code that computed all of the chemical reactions present in the decomposition process. More recently, a multicomponent multi-reaction model that focused on the two main reactions was developed (Asay, et al, 2014): one for the explosive and one for the oxidation of aluminum. Such a model achieved higher accuracy than single reaction models and more computational efficiency than a separate chemical code. Currently the model uses the excess oxidizers from the explosive to fuel the oxidation reaction of the aluminum but ignores any input from the outside air. This paper demonstrates the implementation of the described model in our own 2D axisymmetric hydrocode and adds in mixing along the explosive product boundary to incorporate contributions from the outside air and measure its effects on the oxidation rate of the aluminum.

126* – A Study of Approximation Error in Eulerian Hydrocodes

Parth Y. Patel and David L. Littlefield

In this work we examine a number of approximations for the formulation of Eulerian hydro-codes. These approximations were borne out of an original requirement for the code to run as fast as possible – i.e. with accuracy being secondary to speed. Many of these approximations are originated from the 1970's when computers were slow and memory was at a premium. Although speed and memory are not as much of an issue today, these approximations are still used to formulate the hydrocodes. We examine the effect of these approximations systematically. The lumped mass approximation is an approximation to the consistent mass formulation used in hydrocodes. While the lumped mass approximation is computationally efficient, the consistent mass formulation is the most accurate (and computationally expensive) option. There are other levels of approximation between these two extremes that trade off computational efficiency for accuracy. As is shown in this work, some of these result in tridiagonal systems which are very computationally efficient to solve. Linear finite elements are also used pervasively in hydrocodes. Like the lumped mass approximation, the use of linear elements was borne out of the requirement for computational efficiency and not accuracy. It is indeed surprising linear elements are still used today. In this work higher order finite elements, including quadratic and cubic elements, are examined.

Technical Session 9:

Asteroid Impact and Planetary Defense

(*denotes Poster Session)

038 – Impact Modeling for the Double Asteroid Redirection Test (DART) Mission

Emma S. G. Rainey, Angela M. Stickle, Andrew F. Cheng, Andrew S. Rivkin, Nancy L. Chabot, Olivier S. Barnouin, Carolyn M. Ernst, and the AIDA/DART Impact Simulation Working Group

We present results from numerical simulations of the DART impact using the CTH shock physics code with 2D homogenous asteroid models. A design of experiments approach was used to create a run matrix of 28 simulations varying 17 different material model inputs for the impactor and target. The resulting values of the momentum transfer efficiency factor and the crater width and depth were analyzed to determine the relative sensitivity of each parameter for predicting the DART impact outcome. We found that and crater width/depth ratio are primarily influenced by a small number of material model input parameters, a result which greatly reduces the parameter space required for more expensive 3D simulations.

028 – Momentum Transfer in Hypervelocity Cratering of Meteorites and Meteorite Analogs: Implications for Asteroid Deflection

George J. Flynn, Daniel D. Durda, Mason J. Molesky, Brian A. May, Spenser N. Congram, Colleen L. Loftus, Jacob R. Reagan, Melissa M. Strait, and Robert J. Macke

Porosities of asteroids range from 0 to >50%, with most >20%, and some asteroids exhibit an 0.7 micron water feature in their reflection spectra. Both porosity and hydration are expected to influence the momentum transferred in hypervelocity collisions. We conducted a series of measurements of the post-impact momentum, which is characterized by a factor b, the ratio of the total linear momentum acquired by the target to the momentum of the impactor. We measured b for anhydrous meteorites (samples of their asteroidal parent bodies), spanning a wide range of porosities, including 5 samples of the CV3 carbonaceous chondrite Northwest Africa (NWA) 4502 (2.1% porosity), 7 samples of the ordinary chondrite NWA 869 (6.4% porosity), 4 samples of the ordinary chondrite Saratov (15.6% porosity), and 2 samples of terrestrial pumice (80% porosity), as well as hydrous meteorite analog targets, including 3 samples of terrestrial serpentine (17.9% porosity) and 4 samples of terrestrial montmorillonite (51.5% porosity), the two clay minerals that dominate the composition of the hydrous CI carbonaceous chondrite meteorites, as well as 4 samples of hydrous meteorite analog material prepared by powdering and hydrating an anhydrous carbonaceous chondrite. We found that for both the anhydrous and the hydrous samples b decreased with increasing porosity, consistent with hydrocode modeling. However, the b values we measured for the anhydrous samples are larger, with b = 3.55 for NWA 4502, 2.69 for NWA 869, 2.10 for Saratov, and 2.15 for pumice, than results from hydrocode modeling for 5 km/s impacts into relatively strong, porous rock targets. The b values for the moderate porosity (17.9%) hydrous serpentine target (b = 4.70) and the highly porous (51.55% porosity) hydrous montmorillonite target (b = 2.99) are each more than twice the b value for anhydrous targets of comparable porosities. This is likely due to jetting of water vapor, which could significantly affect the deflection of hydrous asteroids and comets in natural or human-induced collisions.

032 – Simulations of Magnetic Fields Produced by Asteroid Impact: Possible Implications for Planetary Paleomagnetism

David A. Crawford

The origin and evolution of the Moon's magnetic field, specifically whether it has an endogenic or exogenic origin, has been a major question in lunar science. The lunar field today is a patchwork of magnetic anomalies carried as remnant magnetization in the rocks of the lunar crust. Recent publications suggest some magnetic anomalies may be associated with magnetized impact melt sheets of some large lunar basins cooling in the presence of an early lunar core dynamo or associated with portions of the impactor that formed the South Pole-Aitken Basin. By performing CTH simulations of asteroid impacts incorporating magnetic field generation and thermoremanence magnetization models, this paper helps explain the origin of lunar magnetic anomalies by showing: 1) transient magnetic fields produced by impact events will increase to substantial magnitude at the scale of large lunar basins and 2) magnetization of lunar rocks can occur during crater formation at nearly all scales. If occurring in pristine feldspathic lunar highlands rocks with relatively low thermoremanence susceptibility, the magnetic anomalies resulting from (1) and (2) produce magnetic fields observable in orbital magnetic field data only for large and relatively rare impact craters - large lunar basins greater than ~200 km diameter. If occurring in thick units with higher thermoremanence susceptibility, craters as small as 50-100 km may produce orbital anomalies. Craters at nearly all scales may leave behind remnant magnetic fields observable at the surface or in samples. This paper concludes magnetic fields produced by impacts may be an important contributor to the present state of the Moon's magnetic field.

049 – Size Scaling of Crater Size, Ejecta Mass, and Momentum Enhancement Due to Hypervelocity Impacts into 2024-T4 and 2024-T351 Aluminum

James D. Walker, Sidney Chocron, and Donald J. Grosch

Impact tests were performed from 4 to 5.77 km/s of 3.0-cm-diameter aluminum spheres impacting 2024-T351 aluminum targets. It was seen that there are no size-scaling effects for the crater depth. The slight size scaling effect in the crater diameter directly correlated with the nonlinear size-scaling effect in the ejecta mass. There is a qualitative change in the

ejecta mass somewhere in the vicinity of 1.27-cm-diameter impactors, in that less than this the ejecta mass scales with a square root of the impact diameter times impact speed squared, but for larger diameter spheres there is no longer a size dependence and the ejecta mass scales with impact velocity squared. This is likely due to some sort of failure saturation effect, where the size scale is large enough that material damage involving intrinsic length or time is able to completely occur. We show that the 0.45 power dependence on the projectile diameter for the momentum enhancement $\beta - 1$ continues up through the 3.0-cm-diameter sphere impactors, even though there is a qualitative and quantitative change in the ejecta mass behavior.

059 – Hypervelocity Impact on Concrete and Sandstone: Momentum Enhancement from Tests and Hydrocode Simulations

Sidney Chocron, James D. Walker, Donald J. Grosch, Stephen R. Beissel, Daniel D. Durda, and Kevin R. Housen

Concrete, sandstone, and, in a previous round of experiments, pumice, were tested under hypervelocity impact at SwRI. Aluminum spheres with diameters of 1 and 1.75 in were shot at a velocity of approximately 2 km/s using a 50-mm conventional powder gun. The targets were mounted on a swing so that the momentum enhancement could be measured. The size effect, i.e. comparing momentum enhancement generated by the small and large projectiles, was of particular interest in this project. The targets were also scaled, although for sandstone we were limited by the natural geometry of the rocks. The results from the experiments show a clear size effect for the concrete while sandstone did not show any size effect, possibly because of experimental artifacts. The sandstone behavior was investigated with computations using the EPIC hydrocode. The porosity and compressive strength of the sandstone used in the impact tests were measured and reported. The rock is very similar to one reported and extensively tested by Lawrence Livermore Laboratory in 1974. Two material models (Holmquist-Johnson Concrete and Johnson-Holmquist-Beissel) were fit to the data from LLL. The momentum enhancement predicted by the code is reported for different parameter studies.

Technical Session 10:

Material Response II

(*denotes Poster Session)

020 – Statistics of Energy Dissipation in the Hypervelocity Impact Shock Failure Transition

Dennis Grady

In the hypervelocity impact event, shock waves subject material to failure transitions with the attendant dissipation of the imparted energy. Under shock compression, failure and dissipation entail intense inelastic shear and compaction. Through shock interactions, states of dynamic tension are achieved and further failure dissipation involves fracture and fragmentation. The nature of failure of solids in the shock environment has encouraged considerable experimental effort through the past several decades. Such efforts have yielded results that suggest universality in the shock failure response over significant spans of shock intensity. Examples include the fourth-power relation between pressure and strain rate in solid-material compressive shock waves, and power-law relations capturing spall fracture strength and fragmentation size scale in dynamic tensile failure. Comparable power-laws also describe the shock compaction of distended solids. The present paper explores a statistical perspective of the underlying micro failure dynamics for the purpose of achieving better understanding of the macro failure trends noted above. A statistical correlation function description of the random micro velocity field is introduced. Through the attendant kinetic dissipation, the statistical dissipation-fluctuation principle is applied to the shock failure transition. From this statistical approach, power-law relations for compressive and tensile shock failure emerge that replicate the reported experimental behavior. Results are compared with selected experimental data.

042 – Dynamic Response of Graphene and Yttria-stabilized Zirconia (YSZ) Composites

Christopher R. Johnson and John P. Borg

A series of dynamic compaction studies were performed on yttria-stabilized zirconia (YSZ) and graphene composites using uniaxial flyer plate impact experiments. Studies aimed to characterize variation in dynamic behavior with respect to morphological differences for eight powdered YSZ and graphene compositions. Parameters of interest included YSZ particle size (nanometer or micrometer) and added graphene content (graphene weight percentage: 0%, 1%, 3%, 5%). Experiments were performed over impact velocities ranging between 315 and 586 m/s, resulting in pressures between 0.8 and 2.8 GPa. Hugoniot states measured appear to exhibit dependence on particle size and graphene content. Shock velocities tended to increase with graphene content, and were generally larger in magnitude for the micrometer particle size YSZ. Induced strain decreased as graphene content was increased, and was generally larger for the nanometer particle size YSZ samples. Resulting Hugoniot curves are compared and summarized to convey the dynamic behavior of the specimens.

102 – Validating Ice Impacts Using Adaptive Smoothed Particle Hydrodynamics for Planetary Defense

Dawn Graninger, Megan Bruck Syal, J. Michael Owen, and Paul Miller

Understanding how a potentially hazardous object (PHO) responds to a kinetic impactor is of great interest to the planetary defense community. Target response depends upon the detailed material properties of the PHO, which may not be well constrained ahead of time. Hence, it is useful to explore a variety of target compositions for kinetic impact deflection. Previous validation efforts have focused primarily on understanding the behavior of common rocky materials, though PHOs are not exclusively composed of such material. Water ice is one material for which there has been only limited code validation against cratering experiments. It is known that comets consist of primarily icy material and some asteroids likely contain some amount of ice. Therefore, it is useful to understand the model sensitivities for ice in deflection simulations. Here we present Adaptive Smoothed Particle Hydrodynamics simulations of impacts into water ice by an aluminum projectile. We explore the sensitivities to the damage model within our code and find that the best-fit simulations of ice occur with a Weibull modulus of 12, though results can be obtained with values of the Weibull modulus near the published value of 9.59. This work demonstrates though the efficacy of using an adaptive smoothed particle hydrodynamics code to simulate impacts into ice.

007 – Wave Speeds in Single and Polycrystalline Copper

Sarah A. Thomas, Robert S. Hixson, M. Cameron Hawkins, and Oliver T. Strand

A novel technique was used to determine shock speeds in polycrystalline and single crystal copper that makes use of the ready availability of multiple velocimetry channels. Making use of a "top hat" design and five points of photonic Doppler velocimetry (PDV), which allows for accurate timing to determine wave arrival times, shock impacts were executed on [100], [110], and [111] single crystal copper, as well as polycrystalline copper at impact velocities ranging from 300 to 600 m/s. The data show that at these low velocities the [111] and [110] single crystal orientations have different shock speeds than the polycrystalline and [100] single crystal, but those differences may be within the apparent accuracy of the experimental technique.

027 – Study on Phase Transformation in Tin under Dynamic Compression

Camille Chauvin, Frédéric Zucchini, Thierry D'Almeida, and David Palma de Barros

We propose to study experimentally the polymorphic transition of Tin under dynamic compression. These transformations have been investigated for a long time through usual velocity measurements under shock from ambient condition and at CEA Gramat we have improved our understanding of such phase transformations through both experimental and theoritical means. Experimental velocity measurements have long suggested that non equilibrium behavior and kinetics is an important part of the dynamic compression response of materials undergoing phase transformations. Empirical kinetic models can in a lot of cases reproduce the experimental velocity profiles but without clearly identifying the nature of the transition.
For nearly two decades, the CEA Gramat operates several gas guns for shock loading and high pulsed power (HPP) drivers dedicated to Isentropic Compression Experiments (ICE) up to several GPa. These experimental devices associated with diagnostics (velocimetry and temperature measurements and X-ray diffraction experiments) help to begin to study kinetics under dynamic transition in a more rigorous manner verified on various compression paths and contribute to constrain equation of state (EOS) models incorporated in our numerical codes. The latter is usually produced starting from ambient conditions and loading metallic materials from various non ambient initial temperatures can significantly extend the range of our studies into previously unexplored thermodynamic paths. We propose to describe our preheating devices for gas gun experiments and our HPP driver and to present our preliminary results on shock loading and on isentropic compression at various initial temperatures to explore the phase diagram of Tin. Besides, we present the design of a promising testing on x-ray diffraction under shock to help to understand a more physical kinetic model relying on nucleation and growth mechanisms which are implemented in our continuum level codes.

Keynote 2: 047 – High Strain-rate Shear and Friction Characterization of Fully-Dense Polyurethane

Peter Sable, Christopher H. Neel, and John P. Borg

A series of friction and constant-pressure oblique plate impact experiments were conducted in an effort to observe dynamic friction characteristics and shear strength behaviors of fully dense, high durometer polyurethane (PU). For both configurations, an angle-faced projectile was accelerated towards a target set at the same angle via slotted-barrel light-gas gun. Oblique impact resulted in high strain-rate (~105 s-1) combined normal and shear stress loading with magnitudes of approximately 0.9 and 0.2 GPa, respectively, depending on impact velocity and angle. Material response was inferred from rear free-surface particle velocities measured using transverse photon Doppler velocimetry techniques. Coefficients of friction were calculated from the ratios of shear to normal stress at the impact interface between a PU projectile and 7075-T6 aluminum target. Taking into account the slip speed as the difference between expected and observed transverse velocity, the coefficient of friction was ranged from 0.1 to 0.3 with an apparent inverse pressure dependence. Shear strengths were found to gradually increase with confining normal stress, greatly exceeding magnitudes seen by traditional low-rate tensile and shear testing. Additionally, a discussion on the role of adhesion is presented contrasting polymer-metal bond failure to intrinsic material failure.

Technical Session 11:

High Velocity Launchers

(*denotes Poster Session)

016 – Electrically-Launched mm-sized Hypervelocity Projectiles

W. Casey Uhlig, Paul R. Berning, Peter T. Bartkowski, and Matthew J. Coppinger

An electrothermal research gun capable of firing small cylindrical projectiles up to 4 km/s has been developed. While electromagnetic forces certainly exist in the system, it is not an electromagnetic launch system, but rather utilizes an electrical arc to produce a rapidly expanding gas that is used as the working fluid. A pointed copper anode is insulated such that the arc initiates only at the very tip, while the electrical circuit is completed through both the projectile and the barrel. Experiments show that copper vapor from the eroding copper electrode is the most likely working fluid of the gun, however, a portion of the aluminum projectile is also eroded. The design was directly aided by simulations performed using the Multiphysics hydrocode ALEGRA developed by Sandia National Laboratories. Simulations included investigating the anode tip shape as well as limiting the expansion of the chamber due to the rapid expansion of gasses caused by the arc. Comparisons of projectile velocity profiles from Photon Doppler Velocimetry, barrel expansion, and pellet erosion with the ALEGRA results were utilized as benchmarks, leading to significant velocity gains for given energy inputs.

039 – HyFIRE: Hypervelocity Facility for Impact Research at Johns Hopkins University

Gary Simpson, Matthew Shaeffer, and K.T. Ramesh

The Hopkins Extreme Materials Institute (HEMI) recently installed a hypervelocity impact facility (HyFIRE) including a two-stage light gas gun at Johns Hopkins University in Baltimore, MD. The HyFIRE launcher has a launch tube bore diameter of 7.62 mm and is designed to attain launch velocities up to 7 km/s. The enclosed ballistic range and terminal test chamber provide multiple axes with which to view both projectile free flight and terminal impact, maximizing diagnostic access to events of interest. Initial test diagnostics include ultra-high-speed optical video and orthogonal 300 kV flash x-ray imaging. Photon Doppler velocimetry for surface velocity measurement—currently used in HEMI's laser shock facility—as well as emission spectroscopy/pyrometry are planned, providing researchers across multiple disciplines with the ability to investigate the coupling of mechanics, physics and chemistry present in high energy density impact events. Initial experiments at the facility investigate the fragmentation of inert impactors on anvil targets, with an aim towards identifying the dominant mechanisms controlling the fragmentation characteristics, temperature distributions and trajectories of generated debris fields.

084 – The JHUAPL Planetary Impact Lab (PIL): Capabilities and Initial Results

R. Terik Daly, Olivier S. Barnouin, Andrew M. Lennon, Angela M. Stickle, Emma S. Rainey, Carolyn M. Ernst, and Andrew A. Knuth

The Planetary Impact Lab (PIL) at the Johns Hopkins University Applied Physics Laboratory (JHUAPL) includes a single-stage, compressed inert gas gun that can be used for impact experiments. The impact angle can be varied from 15° to 90° with respect to horizontal, a capability which enables oblique impacts into unconsolidated or granular materials (e.g., regolith analogs). The gun currently achieves impact velocities up to 400 m/s, although future enhancements could increase the maximum projectile velocity. Experiments can be done with atmospheric pressures ranging from ambient pressure down to ~75 Pa. The gun uses sabots produced with state-of-the-art additive manufacturing techniques (AM). Several engineering challenges had to be overcome to create a reliable AM sabot; however, AM sabots are ~45% lighter than and provide substantial cost savings over machined sabots. The PIL gun is currently being used to investigate impact processes on sloped coarse-grained surfaces, with application to planetary science and, specifically, rubble-pile asteroids. In contrast to previous studies of impacts onto slopes, we kept the projectile trajectory perpendicular to the target surface, thereby disentangling the effects of oblique impacts from the effects caused by a sloped surface. Initial results show enhanced crater collapse in the sloped target, with most of the collapse occurring in the direction parallel to the surface gradient. Consequently, final craters on sloped targets have smaller volumes and reduced depth-to-diameter ratios.

117 – Timing Analysis of the Auxiliary Pump Technique to Improve the Performance of an Implosion-Driven Hypervelocity Launcher

Mafa Wang, Justin Huneault, Andrew J. Higgins, and Sen Liu

In order to find out the reason why the auxiliary pump technique is irreproducible, an interior ballistic solver taking into account reservoir collapse has been used to simulate the performance of launchers. Launchers with different detonation velocities, explosive lengths, and timings (the difference of initiation time between pump tube explosives and auxiliary pump explosives) of the auxiliary pump have been calculated. Results show that the velocity gain decreases with an increase in timing and increases with the increasing length of explosives. Further analysis shows that the timing delay region for obtaining a gain greater than 0.5 km/s is about 10 μs. This region depends weakly on the detonation velocity and the length of explosives. The timing delay region for a gain larger than1.0 km/s is about 2 μs, which is too small for the auxiliary pump technique to obtain a gain of 1.0 km/s in tests. Therefore, it should not be a very reproducible technique. In addition, the detonation velocity of auxiliary pump explosives and the inner-wall velocity of the reservoir have been further discussed. Results show that low detonation velocity and high inner-wall velocity could enlarge the timing delay region for a gain larger than 1.0 km/s. But the maximum region of a gain of 1.0 km/s will not exceed 10μs. It is still not easy to be realized in tests.

092* – Transitional Ballistics of Electric High-Velocity Launchers

B. Reck , S. Hundertmark, R. Hruschka, A. Zeiner, B. Sauerwein, and M. Schneider

The high-velocity launch of a projectile is subjected to a number of disturbances which exert an influence on the flight trajectory. In the case of sub-caliber projectiles, sabot separation is one of the critical aspects. In this work, we focus on the projectiles and the launch package of an electric railgun launch, i.e. on the behavior of the launch-package, when transitioning from the gun barrel to free-flight. This work further addresses the use of a hydrocode for creating numerical models which are capable of predicting the motion and deflection of the sabot parts during their separation from the projectile after exiting the muzzle. An earlier study showed that the air flow around the projectile and the sabot can be modeled with sufficiently high accuracy by means of a simulation code that uses an Eulerian description of the gas flow. Within a time interval of several milliseconds, just the duration that a projectile needs to enter quasi-stationary flight, viscous effects of the air or gas flow have relatively little influence on the sabot discard process. If the Eulerian gas flow is coupled with the Lagrangian structural parts, the mechanical response of the latter to the gas pressure can be complex in terms of deformation and damage, and in that way, can affect the gas flow. In this study, the hydrocode model is applied to a medium caliber launch package concept for accelerating long rod projectiles. The computed results agree well with the corresponding experimental values obtained from a launch package model test in the shock tunnel at Mach 4.5. This demonstrates that the presented hydrocode model can be used for launch package design optimizations with high confidence.

Technical Session 12:

Spacecraft Meteoroid and Debris Shielding II

(*denotes Poster Session)

037 – Depth of Penetration Criteria on Metallic Surfaces for Use in MMOD Risk Assessment

Henry Nahra, Louis Ghosn, Eric Christiansen, Joshua Miller, and Bruce A. Davis

System-level assessment of hypervelocity impacts by micrometeoroids and orbital debris (MMOD) relies on the definition of the spacecraft geometry and trajectory, the natural environment of the micrometeoroids and induced environment of the orbital space debris, ballistic limit equations and the failure criteria. The definition of the MMOD environments provides the particles flux and when is combined with the ballistic limit equations will determine the number of the critical penetrating particles that could result in the failure of the underlying component is calculated and is used to calculate the risk based on some failure criterion. Spacecraft geometry provides the shielding configuration over the spacecraft critical body which defines the selection of the ballistic limit equations to be used in the risk assessment. The definition of the failure criterion for metallic pressure systems involves the definition of the allowable depth of penetration that could result in leakage or burst of the component. This paper addresses the definition of the allowable depth of penetration of generic metallic tanks from MMOD impacts. The allowable penetration depth of metal tanks is based on a fracture mechanics approach calibrated using biaxially stressed coupons subjected to Hypervelocity Impacts (HVI). The planar crack-crack spacing was based on the craters spacing distribution of the HVI coupon tests. The Stress Intensity Factor (SIF) as a function of crater depths and crater spacing and applied remote stress is calculated using NASGRO®, a linear fracture mechanics software. The calculated SIF is compared with the material fracture toughness to determine if the craters result in a failure of the coupons under biaxial stress. This work resulted in a recommended allowable depth of penetration of 20% on the surfaces of metallic pressure vessels on spacecraft.

071 – Numerical Study of Dynamic Behavior of Foams Subjected to High- to Hyper-Velocity Impact

Xiaotian Zhang, Ruiqing Wang, and Q.M. Li

Hypervelocity tests and numerical studies have been reported in the literatures for aluminum foam to show its potential applications in spacecraft shielding against space debris based on "shielding set-up" Meanwhile the "forward impact" set-up has been widely reported in the literature to study the dynamic behavior of the foam materials in the range of low to intermediate impact velocities. This paper extended the forward impact to high- and hyper-velocity impacts to understand the dynamic deformation and failure mechanisms based on numerical simulation. The focused impact velocity range is from about 1km/s to 6km/s. The cell-based numerical model of the foam material is used along with the Smoothed Particle Hydrodynamics (SPH) method to simulate the deformation and the failure process. The failure of the foam materials in the range of intermediate to high impact velocities is related to the plastic yielding and crushing of the foam cell, while that in the hypervelocity impact is related to the cell material erosion. Dynamic effects in different impact velocity ranges also lead to shock and strain-rate effects. The understanding of the dependence of the deformation/failure mechanisms on the impact velocity helps the application of foam materials in relevant range of impact velocities.

029 – Predicting Orbital Debris-Induced Failure Risk of Wire Harnesses Using SPH Hydrocode Modelling

Joel Williamsen, Michael Squire, and Steven Evans

This Paper Describes A Method Derived To Assess The Probability Of Two Types of complex cable failures, considering their location with respect to the debris spray from penetration of multi-layer insulation (MLI) suspended over them, and the likelihood of impacting particle sizes and velocities as predicted by NASA's model for predicting orbital debris impact size and velocity distributions for satellites in low earth orbit, ORDEM. The smooth particle hydrodynamics (SPH) code was used to determine the onset of these two failure types following hypervelocity impact for different orbital debris velocities, sizes and orientations relative to four different wire locations for a prototypical satellite in a 98-degree polar orbit at an altitude of approximately 750 km (i.e., a typical weather satellite). Interpolations between hydrocode results, combined with ORDEM predictions of orbital debris likelihoods, were used to predict overall risk of two failure types (partial and full wire breaks).

054 – Debris Risk Evolution and Dispersal (DREAD) for Post-Fragmentation Modeling

Daniel L. Oltrogge and David A. Vallado

The Debris Risk Evolution And Dispersal (DREAD) tool facilitates the 3D modeling and risk analysis of the fragmentation cloud after a collision or explosion. This tool uses the NASA Standard Breakup Model and other breakup models "under the hood" that are capable of estimating the Probability Density Function (PDF) of induced relative velocity, mass and area of fragments as a function of object size. DREAD can be further enhanced by incorporation of alternate, more detailed hypervelocity simulations that enforce conservation laws (conservation of mass, angular and linear momentum and kinetic energy). We also discuss our recent incorporation of an improved technique to normalize risk by the expansion volume occupied by debris fragments. DREAD is then used to examine the likely debris fragmentation cloud created by the Fengyun 1C ASAT intercept test conducted by the Chinese in 2007 and the risk it subsequently posed to other spacecraft and the cloud's evolution and dispersal.

026 – A Rupture Limit Equation for COPVs Following a Perforating MMOD Impact

William P. Schonberg

Most spacecraft have at least one pressurized vessel on board. One of the primary design considerations for earth-orbiting spacecraft is the anticipation and mitigation of the possible damage that might occur in the event of a micrometeoroid or orbital debris (MMOD) particle impact. To prevent mission failure and possibly loss of life, protection against perforation by such high-speed impacts must be included. In addition to a hole, it is possible that, for certain pressure vessel designs, materials, impact parameters, and operating conditions, a pressure vessel may experience catastrophic failure (i.e. rupture) as a result of a hypervelocity impact. If such a tank rupture were to occur on-orbit following an MMOD impact, not only could it lead to loss of spacecraft, but quite possibly, for human missions, it could also result in loss of life. In this paper we present an update to a Rupture Limit Equation, or RLE, for composite overwrapped pressure vessels (COPVs) that was presented previously. The update consists of modified RLE parameters and coefficients that were obtained after the RLE was re-derived using new / additional data. The updated RLE functions in a manner similar to that of a ballistic limit equation, or BLE, that is, it differentiates between regions of operating and impact conditions that, given a tank wall perforation, would result in either tank rupture or only a relatively small hole or crack. This is an important consideration in the design of a COPV pressurized tank – if possible, design parameters and operating conditions should be chosen such that additional sizable debris (such as that which would be created in the event of tank rupture or catastrophic failure) is not created as a result of an on-orbit MMOD particle impact.

Technical Session 13:

Analytical and Numerical Methodologies II/Material Response III

(*denotes Poster Session)

109 – Adiabatic Heating and Damage Formation of Composite Associated with High-Velocity Impact

Zhiye Li, Xiaofan Zhang, Daniel J. O'Brien, and Somnath Ghosh

This work aims to develop a physical based multiscale model incorporating material heterogeneities to study multi-physics damage and failure of S-glass fiber reinforced epoxy composites under high-velocity impact.
Micromechanical analysis of unidirectional fibers composites is performed in conjunction with the phenomenon of stress wave propagation in the representative volume elements (RVEs) subjected to high strain rate deformation. Deformation and failure response of RVE model exhibiting fiber and matrix damage as well as cohesive interfacial crack. The rate-dependent nonlocal damage model is validated by DER 353 Epoxy donut impact experiment. From SHPB high-speed impact experiment, thermal softening became more prominent as the strain rate was increased. Adiabatic heating is observed in the donut shape specimens and implemented in the thermos-mechanical damage model. The dynamic rate-dependent cohesive models are validated by the cruciform experiment and micro-droplet experiment. With model parameters calibrated from experiments, characterization of failure properties and microstructure criteria is studied in realistic microstructure models by using a Voronoi cell characteristic method, e.g., cracking nucleation, growth and spacing decrease.

052 – A Mesoscale-Based Statistical Mechanics Framework for Modeling, Homogenization and Uncertainty Quantification of Sand in Hydrocodes

Gerald Pekmezi and David L. Littlefield

This study introduces two important developments in the modeling of granular media. A novel real-time interface tracking algorithm for particle-based simulation methods is the first development. The second development, use

of particle-based simulations in the homogenization and uncertainty quantification (UQ) of granular media, is made possible by the first. The novel interface tracking algorithm uses an advanced surface extraction technique based on the alpha shape paradigm of computational geometry. When used concurrently with particle-based methods, this algorithm is capable of tracking the evolution of the simulation boundaries and applying accurate micro-boundary conditions on them. The micro-boundary conditions may be of Dirichlet type, Neumann type, or mixed-orthogonal type and need not be restricted to scalar pressures. This is a very important development in the modeling of granular media, as it expands the role of particle-based methods for mesoscale simulations within a multiscale framework. The power and versatility of the micro-mechanical boundary tracking algorithm is demonstrated through a series of numerical simulations of sand. The mesoscale models are used to explore the response of sand throughout stress space, including those coordinates that are difficult or even impossible to access in experimental settings. Finally, mathematical optimization is used to calibrate the continuum model (HEP) to the multitude of results provided by the mesoscale simulations.

017 – Mesoscale Modeling and Debris Generation in Hypervelocity Impacts

Stephanie N. Q. Bouchey and Jeromy T. Hollenshead

Material fragmentation after a hypervelocity impact is important to predictive electro-optical and infrared (EO/IR) modeling. Successful comparisons with data require that submicron fragments are generated in such impacts; however, experimental data has so far been unable to produce fragments of this scale. The purpose of this work was therefore to investigate the generation of debris in hypervelocity impacts through sphere-on-plate simulations with the shock physics code, CTH. Specifically, it tested the effect of explicitly modeling the mesoscale grain structure in aluminum with the use of two suites of simulations. The first suite tested the standard isotropic/homogeneous structure and the second study explicitly modeled mesoscale grains and tested the effect on fragment size through the proxy of Grady-Kipp strain rate at failure and material temperature. The isotropic model highlighted findings that demonstrate the underlying physics of the hypervelocity impact problem, whereas the mesoscale grain model explored the effect and sensitivity of a range of key material properties within the grain structure. Comparisons were made between the two simulation suites primarily using histograms and cumulative mass plots of Grady-Kipp strain rate at failure and material temperature. Attempts to change material properties or interface behavior between grains had only a minor effect. Material porosity was the only study to demonstrate an exceptional change in both the Grady-Kipp strain rate at failure and material temperature, but high levels of porosity were used. Shock reflections from voids induced higher strain rates and material temperatures, and similar effects may be produced from inclusions or dislocations in real materials. Thus, interfaces within a material, such as those caused by porosity may play a role in producing smaller debris fragments that support the EO/IR predictive models of hypervelocity impacts.

033 – Hypervelocity Penetration of Granular Silicon Carbide from Mesoscale Simulations

Brian J. Demaske and Tracy J. Vogler

Penetration of gold rods into SiC powder targets at velocities of 1 to 3 km/s are investigated using mesoscale simulations. The range of impact velocities is chosen to coincide with previous penetration experiments. The range of velocities is significantly higher than previous mesoscale simulations and presents a new regime to test their applicability. Both 2D and 3D geometries of the combined penetrator and powder system are considered. Analysis of the penetration depth histories at various impact velocities shows the penetrator undergoes an initial transient period of rapid deceleration within the first few microseconds before converging to a steady state characterized by jumps in the penetration velocity on the order of a few hundred meters per second. Visualization of the material interfaces reveals that these jumps occur when small projections of penetrator material advance in front of the main penetrator-powder interface. Independent of the initial density of the powder bed, average penetration velocities follow a linear relationship with impact velocity with penetration velocities from 2D simulations always lying above those obtained from 3D simulations. The 2D simulations predict a more shallow response in penetration velocity versus impact velocity than observed in experiments, whereas the experimental steepness is correctly predicted by the 3D simulations. For powder beds with roughly the same initial density as experiment, 3D simulations predict a higher penetration resistance, though the agreement can be improved substantially by decreasing the initial density of the simulated powder.

072 – Numerical and Experimental Evaluations of a Glass-Epoxy Composite Material under High Velocity Oblique Impacts

Christopher T. Key and C. Scott Alexander

Composite materials are used as alternatives to conventional metallics in a multitude of applications including military ground vehicles, aircraft, space launch and re-entry vehicles and even personnel protection where weight savings are critical. In application, these materials are susceptible to high velocity impacts from various threats and it is essential that the response of these materials, under relevant conditions, be understood in order to provide optimized effective designs. This work details an on-going effort to validate the anisotropic multiple constituent model (MCM) within the CTH hydrocode. Within the CTH framework, the anisotropic MCM model is coupled with an equation of state (EOS) and provides continuum averaged stress and strain fields for each constituents (fiber and resin) of a composite microstructure from which progressive damage evaluations can be performed. In this paper we focus on recent validation efforts where woven S2/SC15 (glass/epoxy) composite panels were impacted with steel spheres at various impact velocities and angles of obliquity. The experimental testing was performed at the Shock Thermodynamics Applied Research (STAR) Facility at Sandia National Laboratories to provide data for further validation of the MCM model under oblique impact conditions. Oblique impacts result in stress fields which exercise the anisotropy of the strength model and EOS coupling of the MCM model more robustly. Results are presented for both the CTH MCM model predictions and the experimental testing results. The primary comparison metrics evaluated are the predicted and observed damage extent, overall damage pattern, and residual velocity of the sphere.

010 – Effects of EOS and Constitutive Models on Simulating Copper Shaped Charge Jets in ALEGRA

Robert L. Doney, John H. J. Niederhaus, Timothy J. Fuller, and Matthew J. Coppinger

We investigate the effects of copper equations of state and constitutive models on simulations of shaped charge jets using the Sandia National Laboratories' Multiphysics hydrocode, ALEGRA. Specifically, we compare (1) the 3320, 3325, 3331, and 3337 SESAME copper equations of state (EOS), and (2) Johnson-Cook (JC), Zerilli-Armstrong (ZA), Preston-Tonks-Wallace (PTW), Steinberg-Guinan-Lund (SGL), and Mechanical Threshold Stress (MTS) constitutive models. Several of these cases are also compared against photon Doppler velocimetry measurements of the tip velocity. Lagrangian tracer particles are used to follow a part of the jet's evolution in state space for the various models. We monitored the jet topology and found that the various EOS produce similar results, although the 3325 model generates a cavity near the jet tip whose size decreases with increasing mesh resolution. Constitutive models generated more noticeable differences. We found the SGL and PTW models produced higher temperatures while the MTS and JC models returned very similar results at lower temperatures. The SGL model was the only strength model that reported a liquid region along the axis of the jet. For all material models, we found similar results for the velocity history of the jet tip as measured against experiment using photon Doppler velocimetry.

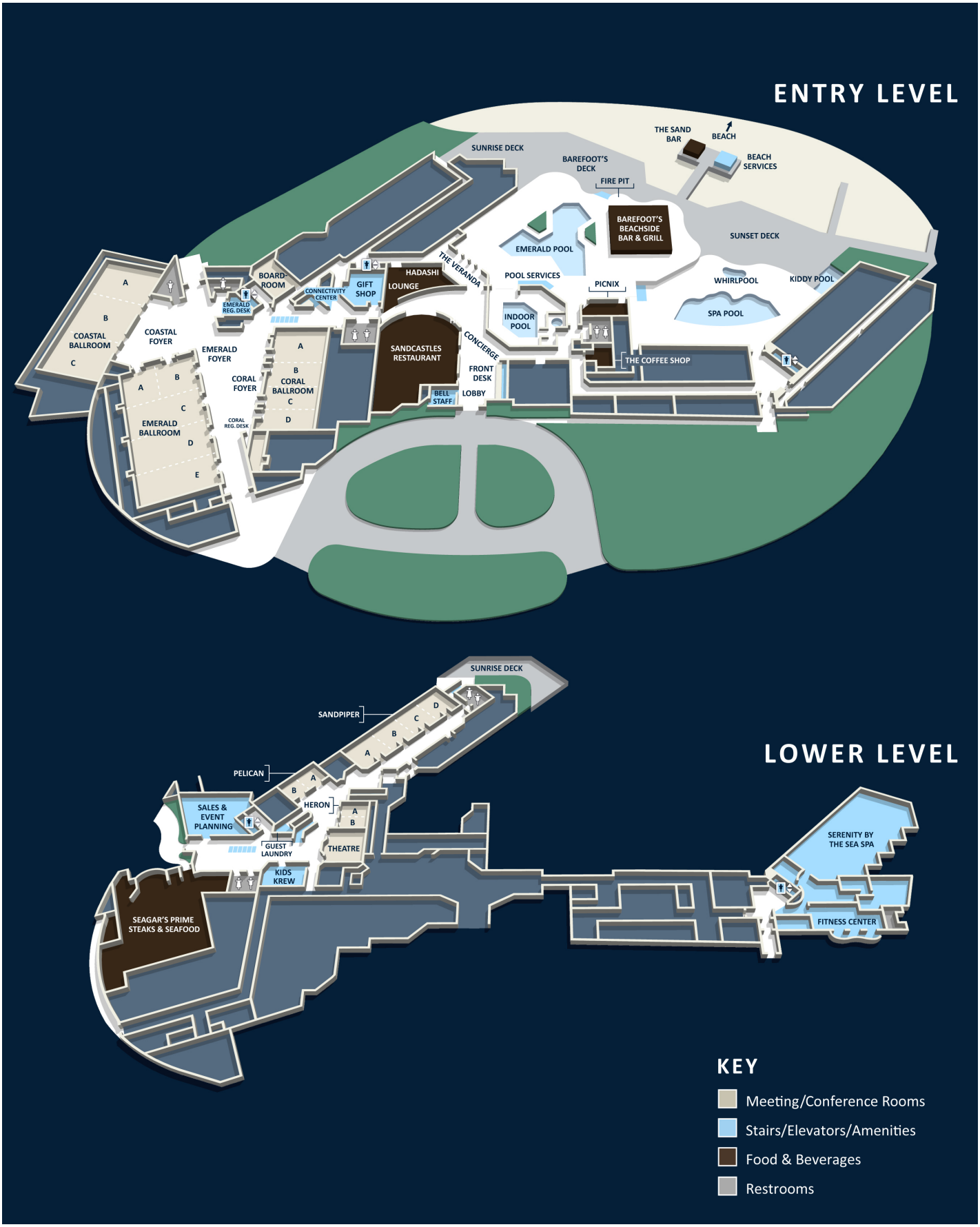
ENTRY LEVEL
THE SAND BAR
BEACH
BEACH SERVICES
SUNRISE DECK
BAREFOOT'S DECK
FIRE PIT
BAREFOOT'S BEACHSIDE BAR & GRILL
SUNSET DECK
EMERALD POOL
THE VERANDA
HADASHI LOUNGE
GIFT SHOP
BOARD ROOM
CONNECTIVITY CENTER
EMERALD REG. DESK
POOL SERVICES
PICNIX
WHIRLPOOL
KIDDY POOL
SPA POOL
INDOOR POOL
COASTAL BALLROOM
COASTAL FOYER
EMERALD FOYER
CORAL FOYER
CORAL BALLROOM
EMERALD BALLROOM
CORAL REG. DESK
SANDCASTLES RESTAURANT
CONCIERGE
FRONT DESK
BELL STAFF
LOBBY
THE COFFEE SHOP
LOWER LEVEL
SUNRISE DECK
SANDPIPER
PELICAN
HERON
SALES & EVENT PLANNING
GUEST LAUNDRY
THEATRE
KIDS KREW
SERENITY BY THE SEA SPA
FITNESS CENTER
SEAGAR'S PRIME STEAKS & SEAFOOD
KEY
Meeting/Conference Rooms
Stairs/Elevators/Amenities
Food & Beverages
Restrooms

Companion Program

Monday, April 15, 2019

Eco Canoe Tour of Walton County's Coastal Dune Lakes

Price per person: $ 50 per person

8:15 am – meet in Lobby, leave from the Hilton Sandestin Resort

Explore beautiful Western Lake home to one of the most eco-diverse places in the world. Experience a 90- minute canoe tour (two people per canoe), guided by Karl, a true naturalist. We will learn about this rare, coastal dune lake, eco system that can only be found here in Walton County, Australia, Madagascar, New Zealand, South Carolina, and Oregon.

Tuesday, April 16, 2019

The Villages of Baytowne Wharf Shopping

Price per person: Complimentary

10 am – meet in Lobby, leave from the resort

12 noon – lunch at Hammerhead's Restaurant (no host)

1:00 pm – leave Baytowne Wharf with group (you are welcome to stay and return to hotel on the Hilton Resort Shuttle as your leisure)

At the Villages of Baytowne Wharf, there is a little something for everyone. This full-service marina and shopping destination is a two-minute shuttle ride across HWY 98 from The Hilton Sandestin. There are boutiques, shopping, restaurants, wave runners, and paddle boards. For children, The Village offers a spacious playground, zip-line, rope course, trail-side tree house, Blast Arcade, and Lazer Maze.

Wednesday, April 17, 2019

Southern Star Dolphin Cruise

Price per person: Adults: $29, Seniors: $25, Children: $15.50

1:15 pm – leave resort in van

2:30 pm – Cruise time

Enjoy a relaxing two-hour tour with Destin's Original Dolphin Cruise on an 80-foot glass bottom boat that has a climate controlled cabin, snacks and gifts available for purchase. Restrooms aboard. Experience up close viewing of dolphins, seabirds and other marine life in their natural habitat in the pristine waters of the Gulf.

Thursday, April 18, 2019

Trip to Seaside

Price per person: Complimentary

9:30 am – meet in Lobby

12 noon – lunch at Bud & Alley's (no host)

2:00 pm – board van and Seaside side streets cruise back to hotel

Seaside is a very unique beach community known for its late 20th century New Urbanest design, as well as pastel-colored houses featuring porches and white picket fences. It's full of shops, restaurants, food trucks and home to a historic, thirty year old post office-the most photographed spot in South Walton other than the beach. The Truman Show was filmed in Seaside.

Things To Do

Serenity by the Sea
The Spa at the Hilton Sandestin Beach
20% off for HIVS Conference Guests
(850) 622-9595

The Shard Shop:
Make-Your-Own Art Boutique
Grayton: (850) 231-0544
Destin: (850) 842-4440

Shopping:

Smith's Antiques Mall and Interior Market
12500 Emerald Coast Parkway, Hwy 98,
Miramar Beach
(850) 654-1484

Grand Boulevard at Sandestin
0.9 miles away from resort
Sandestin's premier entertainment venue includes high-end shops and restaurants, plus a 3-D movie/ dinner theater.

Silver Sands Premium Outlets
Complimentary shuttle service from the resort.

Destin Harbor Boardwalk
10 Harbor Blvd. Fla. 32541

Restaurants:

Captain Dave's (closed Tuesdays)
3796 Scenic Hwy 98, Destin 32541
(850) 837-2627

The Back Porch Seafood & Oyster House
1740 Scenic Hwy 98, Destin 32541
(850) 837-2022

The Crab Trap Seafood & Oyster Bar
3500 Scenic Hwy 98 East, Destin 32541
(850) 654-2722

Surf Hut
551 Scenic Hwy 98, Miramar Beach 32550
(850) 460-7750

Pompano Joe's Seafood House
2237 Hwy 2378, Miramar Beach 32550
(850) 837-2224

McGuire's Irish Pub
Have the Senate Bean Soup – only 18 cents
33 Us-98, Destin 32541
(850) 650-0000

Fudpucker's Bar & Grill
see live alligators
20001 Emerald Coast Pkwy, Destin 32541
(850) 654-4200

The Donut Hole
8 min from resort
6745 US-98, Santa Rosa 32459
(850) 267-3239

SATURN
for MEASUREMENT AND CONTROL

Transient Recorder
Fast Data Acquisition

- Full range of sample rates (kS/s .. GS/s)
- 1..240 analog inputs
- Ready to use analysis & reports
- Digital fiber-optic isolation (option)

Hypervelocity
Impact Prediction

- Combines precise data acquisition and trigger control for high-speed cameras & flashes
- Multi sensor velocity detection
- Individually delayed trigger signals

Sequence Timer
Precision Test Control

- Flexible 8..192 control outputs
- Easy-to-use software
- Digital fiber-optic isolation (option)
- High power switch capability (Options: RELAY, MOSFET, IGBT, SSR, etc.)

AMO tronics

E-Mail: info@amotronics.de
Phone: + 49 241 169780 28

www.amotronics.de

---

nac IMAGE TECHNOLOGY

Stop by booth #9 and see the industry's fastest high speed video camera the MEMRECAM ACS offering 40 GPX of throughput

1,280 X 896 (megapixel resolution) at 40,000 fps

High sensitivity 50,000 ISO

Large memory capacity up to 256 GB

MEMRECAM ACS-1

UV & Visible Options
200M fps
UHSi

UV & Visible Options
1Bn fps
UBSi

Up to a true 1 Billion frames per second

1ns (optically calibrated) Gating and Interframe

12 (optionally 24) Independently Programmed Frames

S25 (Visible) and S20 (UV) versions available

Megapixel Performance

UV to NIR spectral response

Fast Gating to 5ns

High Gain/Sensitivity

Frames rates to > 1,000,000 fps with HSV

Up to 20,000,000 fps in burst mode 100 frame

Integral control panel and external USB control

Exceptional resolution to > 75 lp/mm on SUVi

UVi Camera Intensifier

www.nacinc.com 1 800 969 2711

Optical Velocimetry - PDV Measurements

State-of-the-art, high temporal precision velocity measurements for compact, lower cost laser-based velocimetry.

Single-slot DopplerPXIe module

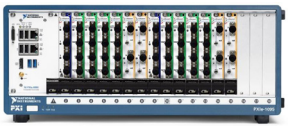

8-channel Homodyne PDV configuration in an 18-slot PXIe chassis

- Drastically reduce the cost and footprint of PDV test.
- Optical management contained in a single PXI slot.
- Minimise the number of manual optical connections and increase repeatability.
- Supports homodyne and frequency-shifted heterodyne PDV testing.
- Built on open-standard PXIe.

Photonics test and measurement solutions

PXI optical test modules
Modular test and measurement

- Laser sources
- Optical spectrum analyzers
- Variable optical attenuators
- Optical-electrical converters
- Optical switches
- Power meters

matrIQ™ Series
Compact USB instruments

The power of all our PXIe optical test instruments in compact, stackable USB/Ethernet benchtop units.

epIQ™ Series
Versatile benchtop solutions

- 4 channel Bit Error Rate Tester
- 4-channel sampling oscilloscope
- Tunable swept laser source

Coherent Solutions is a world-leader in photonics test and measurement. Our portfolio of benchtop and modular test instruments is rapidly expanding to meet the needs of scientists, engineers and manufacturers around the world. Let us work with you to solve your complex problems.

www.coherent-solutions.com

coherent solutions
complexity made simple.

CertaSim www.certasim.com

IMPETUS driving precision

Hypervelocity Impact

"Next Generation" Software and Hardware

IMPETUS γSPH ▪ GPU Technology

Viper Shape Charge

11.8 Million Particles (Runtime 8 hr 6 min)

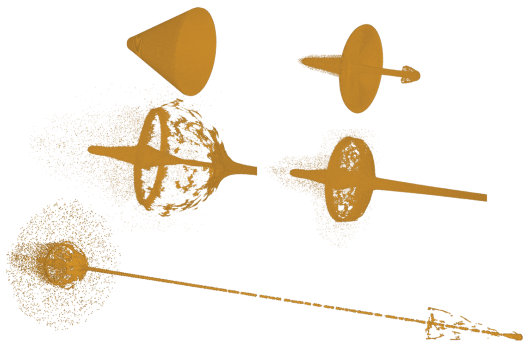

IMPETUS AFEA | SOLVER®

Notes:

Notes:

HYPERVELOCITY IMPACT SOCIETY

UAB

SCHOOL OF ENGINEERING

The University of Alabama at Birmingham